

How Deep Neural Networks Learn Compositional Data: The Random Hierarchy Model

Francesco Cagnetta^{a†*}, Leonardo Petrini^{a*}, Umberto M. Tomasini^a, Alessandro Favero^{a,b}, and
Matthieu Wyart^{a†}

^aInstitute of Physics, EPFL, Lausanne, Switzerland

^bInstitute of Electrical Engineering, EPFL, Lausanne, Switzerland

January 11, 2024

Abstract

Deep learning algorithms demonstrate a surprising ability to learn high-dimensional tasks from limited examples. This is commonly attributed to the depth of neural networks, enabling them to build a hierarchy of abstract, low-dimensional data representations. However, how many training examples are required to learn such representations remains unknown. To quantitatively study this question, we introduce the Random Hierarchy Model: a family of synthetic tasks inspired by the hierarchical structure of language and images. The model is a classification task where each class corresponds to a group of high-level features, chosen among several equivalent groups associated with the same class. In turn, each feature corresponds to a group of sub-features chosen among several equivalent ones and so on, following a hierarchy of composition rules. We find that deep networks learn the task by developing internal representations invariant to exchanging equivalent groups. Moreover, the number of data required corresponds to the point where correlations between low-level features and classes become detectable. Overall, our results indicate how deep networks overcome the *curse of dimensionality* by building invariant representations, and provide an estimate of the number of data required to learn a hierarchical task.

Deep learning methods exhibit superhuman performances in areas ranging from image recognition [1] to Go-playing [2]. However, despite these accomplishments, we still lack a fundamental understanding of their working principles. Indeed, Go configurations and images lie in high-dimensional spaces, which are hard to sample due to the *curse of dimensionality* [3]: the distance δ between neighboring data points decreases very slowly with their number P , as $\delta = \mathcal{O}(P^{-1/d})$ where d is the space dimension. Solving a generic task such as regression of a continuous function [4] requires a small δ , implying that P must be *exponential* in the dimension d . Such a number of data is unrealistically large: for example, the benchmark dataset ImageNet [5], whose effective dimension is estimated to be ≈ 50 [6], consists of only $\approx 10^7$ data, significantly smaller than $e^{50} \approx 10^{20}$. This immense difference implies that learnable tasks are not generic, but highly structured. What is then the nature of this structure, and why are deep learning methods able to exploit it?

A popular idea attributes the efficacy of these methods

to their ability to build a useful representation of the data, which becomes increasingly complex across the layers [7]. Interestingly, a similar increase in complexity is also found in the visual cortex of the primate brain [8, 9]. In simple terms, neurons closer to the input learn to detect simple features like edges in a picture, whereas those deeper in the network learn to recognize more abstract features, such as faces [10, 11]. Intuitively, if these representations are also invariant to aspects of the data unrelated to the task, such as the exact position of an object in a frame for image classification [12], they may effectively reduce the dimensionality of the problem and make it tractable. This view is supported by several empirical studies of the hidden representations of trained networks. In particular, measures such as (i) the mutual information between such representations and the input [13, 14], (ii) their intrinsic dimensionality [15, 16], and (iii) their sensitivity toward transformations that do not affect the task (e.g., smooth deformations for image classification [17, 18]), all eventually decay with the layer depth. However, none of these studies addresses the *sample complexity*, i.e., the number of training data necessary for learning such representations, and thus the task.

*Equal contribution.

†Correspondence to francesco.cagnetta@epfl.ch and matthieu.wyart@epfl.ch.

In this paper, we study the relationship between sample complexity, depth of the learning method, and structure of the data by focusing on tasks with a hierarchically compositional structure—arguably a key property for the learnability of real data [19–26]. To provide a concrete example, consider a picture that consists of several high-level features like face, body, and background. Each feature is composed of sub-features like ears, mouth, eyes, and nose for the face, which can be further thought of as combinations of low-level features such as edges. Recent studies have revealed that deep networks can represent hierarchically compositional functions with far fewer parameters than shallow networks [22], implying an information-theoretic lower bound on the sample complexity which is only *polynomial* in the input dimension [25]. While these works offer important insights, they do not characterize the performance of deep neural networks trained with gradient descent.

We investigate this question by adopting the physicist’s approach [27–30] of introducing a model of synthetic data, which is inspired by the structure of natural problems, yet is simple enough to be investigated systematically. This model (Section 1) belongs to a family of hierarchical classification problems where the class labels generate the input data via a hierarchy of composition rules. These problems were introduced to highlight the importance of input-to-label correlations for learnability [20] and were found to be learnable via an iterative clustering algorithm [23]. Under the assumption of randomness of the composition rules, we show empirically that shallow networks suffer from the curse of dimensionality (Section 2), whereas the sample complexity P^* of deep networks (both convolutional networks and multi-layer perceptrons) is only polynomial in the size of the input. More specifically, with n_c classes and L composition rules that associate m equivalent low-level representations to each class/high-level features, $P^* \simeq n_c m^L$ asymptotically in m (Section 2).

Furthermore, we find that P^* coincides with both *a*) the number of data that allows for learning a representation that is invariant to exchanging the m semantically equivalent low-level features (Subsection 2.1) and *b*) the size of the training set for which the correlations between low-level features and class label become detectable (Section 3). We prove for a simplified architecture trained with gradient descent that *a*) and *b*) must indeed coincide. Via *b*), P^* can be derived analytically under our assumption of randomness of the composition rules.

1 The Random Hierarchy Model

In this section, we introduce our generative model, which can be thought of as an L -level context-free grammar—a generative model of language from formal language the-

ory [31]. The model consists of a set of class labels $\mathcal{C} \equiv \{1, \dots, n_c\}$ and L disjoint vocabularies $\mathcal{V}_\ell \equiv \{a_1^\ell, \dots, a_{v_\ell}^\ell\}$ of low- and high-level features. As illustrated in Fig. 1, left panel, data are generated from the class label α , which is picked uniformly at random from \mathcal{C} . The label generates m high-level representations via m rules of the form

$$\alpha \mapsto \mu_1^{(L)}, \dots, \mu_s^{(L)} \quad \text{for } \alpha \in \mathcal{C} \text{ and } \mu_i^{(L)} \in \mathcal{V}_L, \quad (1)$$

having size $s > 1$. The s elements of these representations are high-level features $\mu_i^{(L)}$ such as background, face, and body for a picture. Each high-level feature generates in turn m lower-level representations via other m rules,

$$\mu^{(\ell)} \mapsto \mu_1^{(\ell-1)}, \dots, \mu_s^{(\ell-1)} \quad \text{for } \mu^{(\ell)} \in \mathcal{V}_\ell, \mu_i^{(\ell-1)} \in \mathcal{V}_{\ell-1}, \quad (2)$$

from $\ell = L$ down to $\ell = 1$. Since the total size of the data increases by a factor s at each level, the input data are made of s^L input features $\mu^{(1)}$, such as the edges in an image. We adopt a one-hot encoding of these features: each of the input elements is a v_1 -dimensional sequence with a single 1 and $v_1 - 1$ 0’s, the index of the 1 representing the encoded feature. As a result, the input data are $s^L \times v_1$ -dimensional.

Note that, for each level ℓ , there are m distinct rules emanating from the same higher-level feature $\mu^{(\ell)}$, i.e., there are m equivalent lower-level representations of $\mu^{(\ell)}$ (see Fig. 1, right panel, for an example with $m = 3$). Following the analogy with language, we refer to these equivalent representations as *synonyms*. In addition, we assume that a single low-level representation can only be generated by one high-level feature, i.e., that there are no ambiguities. Since there are only v_ℓ^s possible representations at level ℓ , this assumption requires $mv_{\ell+1} \leq v_\ell^s$, for all $\ell = 1, \dots, L - 1$ and $mn_c \leq v_L$. Because of synonyms, the number of data per class is exponential in d ,

$$m \times m^s \times \dots \times m^{s^{L-1}} = m^{\sum_{i=0}^{L-1} s^i} = m^{\frac{d-1}{s-1}}. \quad (3)$$

We keep both the representation size s and the number of synonyms m constant throughout the levels for ease of exposition, but all of our results can be generalized with no additional effort. Likewise, we assume that the vocabulary size is constant and equal to v for all levels. Note that, if $m = 1$, each label is represented by a single datum and the model is trivial. By contrast, in the case where $n_c = v$ and $m = v^{s-1}$, the model generates all the possible v^d input data. In the intermediary case $1 < m < v^{s-1}$, the distribution of the inputs has itself a hierarchical structure.

Hence, a single classification task is specified by L sets of rules and can be represented as a s -ary tree, highlighting that the label $\alpha(x)$ of an input datum x can be written as a hierarchical composition of L local functions of s variables [21, 22]. For instance, with $s = L = 2$ (input $x = (x_1, x_2, x_3, x_4)$),

$$\alpha(x_1, \dots, x_4) = g_2(g_1(x_1, x_2), g_1(x_3, x_4)), \quad (4)$$

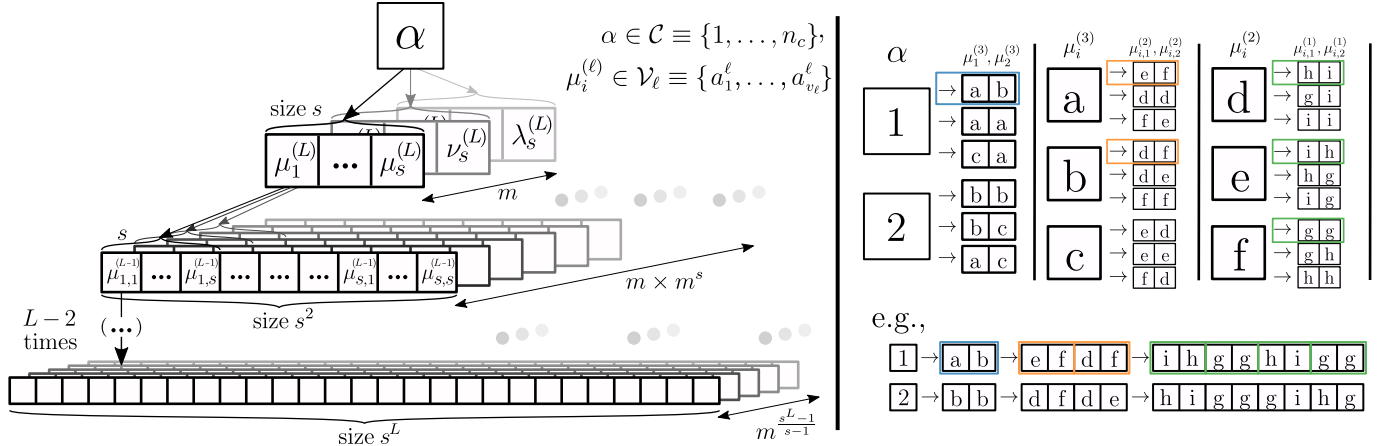


Figure 1: **The Random Hierarchy Model.** **Left:** Structure of the generative model. The class label $\alpha = 1, \dots, n_c$ generates a set of m equivalent (i.e., *synonymic*) high-level representations with elements taken from a vocabulary of high-level features \mathcal{V}_L . Similarly, high-level features generate m equivalent lower-level representations, taken from a vocabulary \mathcal{V}_{L-1} . Repeating this procedure $L - 2$ times yields all the input data with label α , consisting of low-level features taken from \mathcal{V}_1 . **Right:** example of Random Hierarchy Model with $n_c = 2$ classes, $L = 3$, $s = 2$, $m = 3$ and homogeneous vocabulary size $v_1 = v_2 = v_3 = 3$. The three sets of rules are listed at the top, while two examples of data generation are shown at the bottom. The first example is obtained by following the rules in the colored boxes.

where g_1 and g_2 represent the 2 composition rules. In the *Random Hierarchy Model* (RHM) the L composition rules are chosen uniformly at random over all the possible assignments of m representations of s low-level features to each high-level feature. An example of binary classification task ($n_c = 2$), with $s = 2$, $L = 3$, and $v = m = 3$, is shown in Fig. 1, right panel, together with two examples of label-input pairs. Notice that the random choice induces correlations between low- and high-level features. In simple terms, each of the high-level features—e.g., the level-2 features d , e or f in the figure—is more likely to be represented with a certain low-level feature in a given position—e.g., i on the right for d , g on the right for e and h on the right for f . These correlations are crucial for our predictions and are analyzed in detail in [Supplementary Section B](#).

2 Sample Complexity of Deep Neural Networks

The main focus of our work is the answer to the following question.

Q: *How much data is required to learn a typical instance of the Random Hierarchy Model with a deep neural network?*

Thus, after generating an instance of the RHM with fixed parameters n_c , s , m , v , and L , we train neural networks of varying depth with stochastic gradient descent (SGD) on P

training points selected at random among the RHM data. Further details of the specific architectures considered and the training procedure are in the [Methods](#) section.

Shallow networks are cursed. Let us begin with the sample complexity of two-layer fully-connected networks. As shown in Fig. 2, in the maximal case $n_c = v$, $m = v^{s-1}$ these networks learn the task only if trained on a significant fraction of the total number of data P_{\max} . From Eq. (3),

$$P_{\max} = n_c m^{\frac{d-1}{s-1}}, \quad (5)$$

which equals v^{sL} in the maximal case. The bottom panel of Fig. 2, in particular, highlights that the number of training data required for having a test error $\epsilon \leq 0.7 \epsilon_{\text{rand}}$, with $\epsilon_{\text{rand}} = 1 - n_c^{-1}$ denoting the error of a random guess of the label, is proportional to P_{\max} . This is an instance of the curse of dimensionality.

Deep networks break the curse. For networks having a depth larger than that of the RHM L , the test error displays a sigmoidal behavior as a function of the training set size. This finding is illustrated in the top panels of Fig. 3 and Fig. 4 (see [Supplementary Fig. 4](#) of [Supplementary Section G](#) for varying n_c) for Convolutional Neural Networks (CNNs) of depth $L+1$ (further details in [Methods](#)). Similar results are obtained for multi-layer perceptrons, as shown in [Supplementary Fig. 5](#) of [Supplementary Section G](#). All these results suggest the existence of a well-defined number of training data at which the task is learned. Mathematically, we define the sample complexity P^* as the smallest

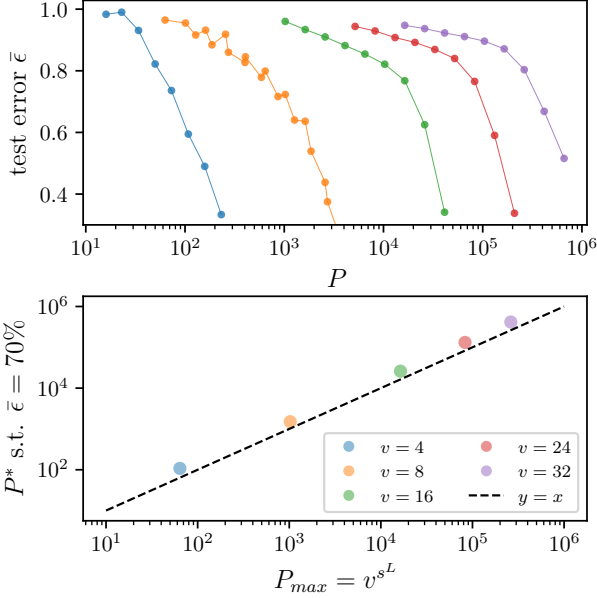


Figure 2: **Sample complexity of two-layer fully-connected networks, for $L = s = 2$ and $v = n_c = m$.** Top: Test error vs the number of training data. Different colors correspond to different vocabulary sizes v . Bottom: number of training data resulting in test error $\bar{\epsilon} = 0.7$ as a function of P_{max} , with the black dashed line indicating a linear relationship.

training set size P such that the test error $\epsilon(P)$ is smaller than $\epsilon_{rand}/10$. The bottom panels of Fig. 3 and Fig. 4 (and Supplementary Fig. 4, Supplementary Fig. 5 of Supplementary Section G) show that

$$P^* \simeq n_c m^L \Leftrightarrow \frac{P^*}{n_c} \simeq d^{\ln(m)/\ln(s)}, \quad (6)$$

independently of the vocabulary size v . Since P^* is a power of the input dimension $d = s^L$, the curse of dimensionality is beaten, which evidences the ability of deep networks to harness the hierarchical compositionality of the task. Hence, we now turn to study the internal representations of trained networks and the mechanism that they employ to solve the task.

2.1 Emergence of Synonymic Invariance in Deep CNNs

A natural approach to learning the RHM would be to identify the sets of s -tuples of input features that correspond to the same higher-level feature, i.e., synonyms. Identifying synonyms at the first level would allow for replacing each s -dimensional patch of the input with a single symbol, reducing the dimensionality of the problem from s^L to s^{L-1} . Repeating this procedure L times would lead

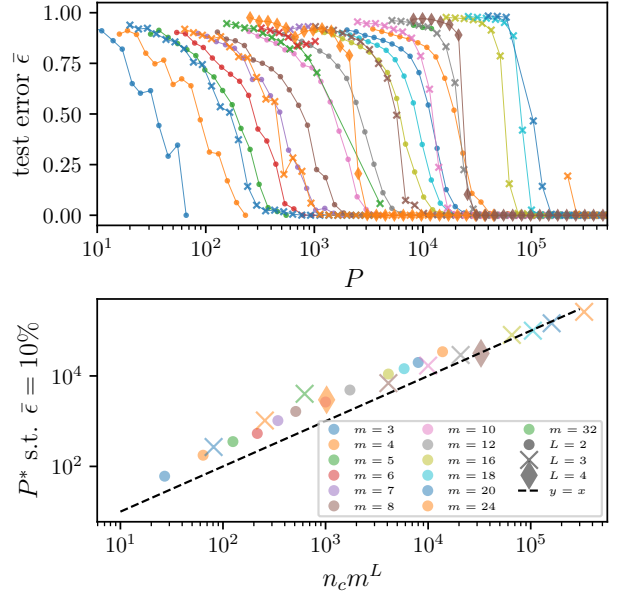


Figure 3: **Sample complexity of deep CNNs, for $s = 2$ and $m = n_c = v$.** Top: Test error vs number of training points. Different colors correspond to different vocabulary sizes v while the markers indicate the hierarchy depth L . Bottom: sample complexity P^* corresponding to a test error $\epsilon^* = 0.1\epsilon_{rand}$. The empirical points show remarkable agreement with the law $P^* = n_c m^L$, shown as a black dashed line.

to the class labels and, consequently, to the solution of the task.

To test if deep networks trained on the RHM resort to a similar solution, we introduce the *synonymic sensitivity*, which is a measure of the invariance of a function with respect to the exchange of synonymic low-level features. Mathematically, we define $S_{k,l}$ as the sensitivity of the k -th layer representation of a deep network with respect to exchanges of synonymous s -tuples of level- l features. Namely,

$$S_{k,l} = \frac{\langle \|f_k(x) - f_k(P_l x)\|^2 \rangle_{x, P_l}}{\langle \|f_k(x) - f_k(z)\|^2 \rangle_{x, z}}, \quad (7)$$

where: f_k is the sequence of activations of the k -th layer in the network; P_l is an operator that replaces all the level- l tuples with one of their $m - 1$ synonyms chosen uniformly at random; $\langle \cdot \rangle$ with subscripts x, z denotes average over all the input data of an instance of the RHM; the subscript P_l denotes average over all the exchanges of synonyms.

Fig. 5 reports $S_{2,1}$, which measures the sensitivity to exchanges of synonymic tuples of input features, as a function of the training set size P for Deep CNNs trained on RHMs with different parameters. We focused on $S_{2,1}$ —the sensitivity of the second layer of the network—since invariance for exchanges of level- l synonyms can generally be achieved

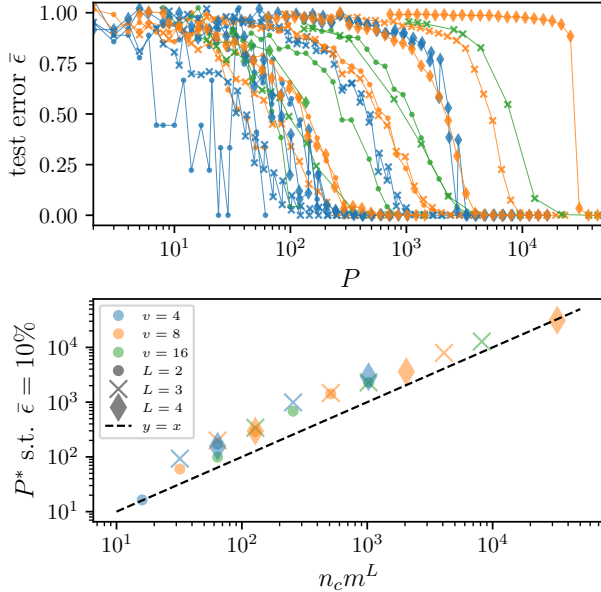


Figure 4: **Sample complexity of deep CNNs, for $s = 2$, $n_c = v$ and varying $m \leq v$.** Top: Test error vs number of training points, with different colors corresponding to different vocabulary sizes v and markers indicating the hierarchy depth L . Bottom: sample complexity P^* , with the law $P^* = n_c m^L$ shown as a black dashed line.

at layers $k \geq l + 1$.¹ Notice that all the curves display a sigmoidal shape, signaling the existence of a characteristic sample size which marks the emergence of synonymic sensitivity in the learned representations. Remarkably, by rescaling the x -axis by the sample complexity of Eq. (6) (bottom panel), curves corresponding to different parameters collapse. We conclude that the generalization ability of a network relies on the synonymic invariance of its hidden representations.

Measures of the synonymic sensitivity $S_{k,1}$ for different layers k are reported in Fig. 6 (blue lines), showing indeed that the layers $k \geq 2$ become insensitive to exchanging level-1 synonyms. Fig. 6 also shows the sensitivities to exchanges of higher-level synonyms: all levels are learned together as P increases, and invariance to level- l exchanges is achieved from layer $k = l + 1$, as expected. The test error is also shown (gray dashed) to further emphasize its correlation with synonymic invariance.

¹This is due to the high probability of overlap between non-synonymic patches. For instance, the low-level representation (h, g) of level-2 feature e in Fig. 1, right panel overlaps with two representations of f ((g, g) and (h, h)). As a consequence, the representations associated with e and f are not linearly separable.

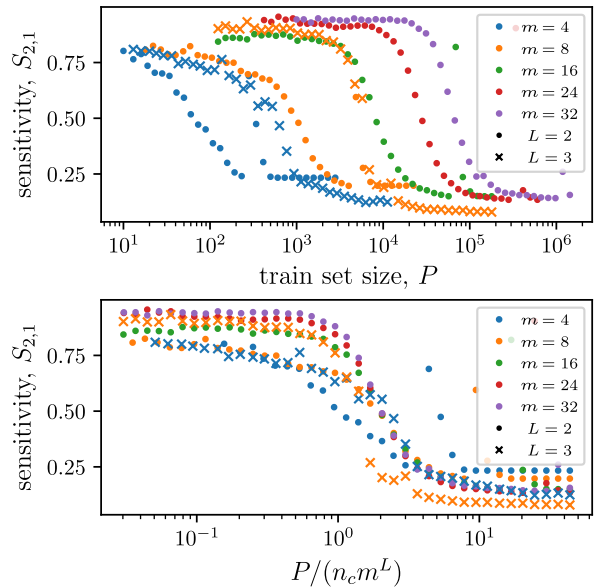


Figure 5: **Synonymic sensitivity $S_{2,1}$ for a deep CNN trained on the RHM with $s = 2$, $n_c = m = v$ as a function of the training set size (L and v as in the key).** The collapse achieved after rescaling by $P^* = n_c m^L$ highlights that the sample complexity coincides with the number of training points required to build internal representations invariant to exchanging synonyms.

3 Correlations Govern Synonymic Invariance

We now provide a theoretical argument for understanding the scaling of P^* of Eq. (6) with the parameters of the RHM. First, we compute a third characteristic sample size P_c , defined as the size of the training set for which the *local* correlations between any of the input patches and the label become detectable. Remarkably, P_c coincides with P^* of Eq. (6). Secondly, we demonstrate how a shallow (two-layer) neural network acting on a single patch can use such correlation to build a synonymic invariant representation in a single step of gradient descent so that P_c and P^* also correspond to the emergence of an invariant representation.

3.1 Identify Synonyms by Counting

Groups of input patches forming synonyms can be inferred by counting, at any given location, the occurrences of such patches in all the data corresponding to a given class α . Indeed, tuples of features that appear with identical frequencies are likely synonyms. More specifically, let us denote \mathbf{x}_j an s -dimensional input patch for j in $1, \dots, s^{L-1}$, a s -tuple of input features with $\boldsymbol{\mu} = (\mu_1, \dots, \mu_s)$, and the

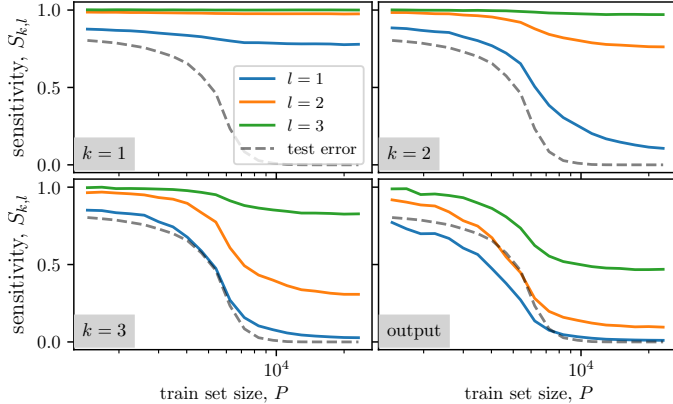


Figure 6: **Synonymic sensitivities** $S_{k,l}$ of the layers of a deep CNN trained on a RHM with $L=3$, $s=2$, $n_c=m=v=8$, as a function of the training set size P . The colors denote the level of the exchanged synonyms (as in the key), whereas different panels correspond to the sensitivity of the activations of different layers (layer index in the gray box). Synonymic invariance is learned at the same training set size for all layers, and invariance to level- l exchanges is obtained from layer $k=l+1$.

number of data in class α having $\mathbf{x}_j = \boldsymbol{\mu}$ with $N_j(\boldsymbol{\mu}; \alpha)$.² Normalizing this number by $N_j(\boldsymbol{\mu}) = \sum_{\alpha} N_j(\boldsymbol{\mu}; \alpha)$ yields the conditional probability $f_j(\alpha|\boldsymbol{\mu})$ for a datum to belong to class α conditioned on displaying the s -tuple $\boldsymbol{\mu}$ in the j -th input patch,

$$f_j(\alpha|\boldsymbol{\mu}) := \Pr\{\mathbf{x} \in \alpha | \mathbf{x}_j = \boldsymbol{\mu}\} = \frac{N_j(\boldsymbol{\mu}; \alpha)}{N_j(\boldsymbol{\mu})}. \quad (8)$$

If the low-level features are homogeneously spread across classes, then $f = n_c^{-1}$, independently of α , $\boldsymbol{\mu}$, and j . In contrast, due to the aforementioned correlations, the probabilities of the RHM are all different from n_c^{-1} —we refer to this difference as *signal*.³ Distinct level-1 tuples $\boldsymbol{\mu}$ and $\boldsymbol{\nu}$ yield a different f (and thus a different signal) with high probability unless they share the same level-2 representation. Therefore, this signal can be used to identify synonymous level-1 tuples.

3.2 Signal vs Sampling Noise

When measuring the conditional class probabilities with only P training data, the occurrences in the right-hand side of Eq. (8) are replaced with empirical occurrences, which

²The notation $\mathbf{x}_j = \boldsymbol{\mu}$ means that the elements of the patch \mathbf{x}_j encode the tuple of features $\boldsymbol{\mu}$.

³Cases in which all features are homogeneously spread across classes can in principle occur in our model due to the randomness of the rules, but their probability vanishes for large m as shown in Supplementary Section E. For such cases, even deep networks are cursed by the input dimensionality, as also shown in Supplementary Section E.

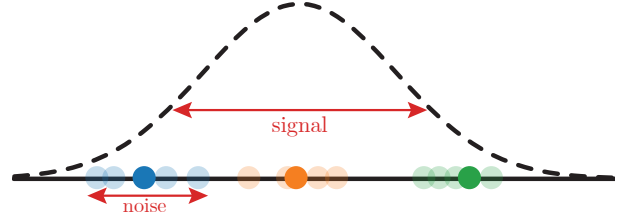


Figure 7: **Signal vs noise illustration.** The dashed function represents the distribution of $f(\alpha|\boldsymbol{\mu})$ resulting from the random sampling of the RHM rules. The solid dots illustrate the *true* frequencies $f(\alpha|\boldsymbol{\mu})$ sampled from this distribution, with different colors corresponding to different groups of synonyms. The typical spacing between the solid dots, given by the width of the distribution, represents the *signal*. Transparent dots represent the empirical frequencies $\hat{f}_j(\alpha|\boldsymbol{\mu})$, with dots of the same color corresponding to synonymous features. The spread of transparent dots of the same color, which is due to the finiteness of the training set, represents the *noise*.

induce a sampling *noise* on the f 's. For the identification of synonyms to be possible, this noise must be smaller in magnitude than the aforementioned signal—a visual representation of the comparison between signal and noise is depicted in Fig. 7.

The magnitude of the signal can be computed as the ratio between the standard deviation and mean of $f_j(\alpha|\boldsymbol{\mu})$ over realizations of the RHM. The full calculation is presented in Supplementary Section B: here we present a simplified argument based on an additional independence assumption. Given a class α , the tuple $\boldsymbol{\mu}$ appearing in the j -th input patch is determined by a sequence of L choices—one choice per level of the hierarchy—of one among m possible lower-level representations. These m^L possibilities lead to all the mv distinct input s -tuples. $N_j(\boldsymbol{\mu}; \alpha)$ is proportional to how often the tuple $\boldsymbol{\mu}$ is chosen— $m^L/(mv)$ times on average. Under the assumption of independence of the m^L choices, the fluctuations of $N_j(\boldsymbol{\mu}; \alpha)$ relative to its mean are given by the central limit theorem and read $(m^L/(mv))^{-1/2}$ in the limit of large m . If n_c is sufficiently large, the fluctuations of $N_j(\boldsymbol{\mu})$ are negligible in comparison. Therefore, the relative fluctuations of f_j are the same as those of $N_j(\boldsymbol{\mu}; \alpha)$, and the size of the signal is $(m^L/(mv))^{-1/2}$.

The magnitude of the noise is given by the ratio between the standard deviation and mean, over independent samplings of a training set of fixed size P , of the empirical conditional probabilities $\hat{f}_j(\alpha|\boldsymbol{\mu})$. Only $P/(n_c mv)$ of the training points will, on average, belong to class α while displaying feature $\boldsymbol{\mu}$ in the j -th patch. Therefore, by the convergence of the empirical measure to the true probability, the sampling fluctuations of \hat{f} relative to the mean are of order $[P/(n_c mv)]^{-1/2}$ —see Supplementary Section B for details. Balancing signal and noise yields the characteristic

P_c for the emergence of correlations. For large m , n_c and P ,

$$P_c = n_c m^L, \quad (9)$$

which coincides with the empirical sample complexity of deep CNNs discussed in [Section 2](#).

3.3 Learning Synonymic Invariance With Gradient Descent

To complete the argument, we consider a simplified one-step gradient descent setting [32, 33], where P_c marks the number of training examples required to learn a synonymic invariant representation. In this setting (details presented in [Supplementary Section C](#)), we train a two-layer fully-connected network on the first s -dimensional patches of the data. This network cannot fit data which have the same features on the first patch while belonging to different classes. Nevertheless, the hidden representation of the network can become invariant to exchanges of synonymous patches.

More specifically, as we show in [Supplementary Section C](#), with identical initialization of the hidden weights and orthogonalized inputs, the update of the hidden representation $f_h(\boldsymbol{\mu})$ of the s -tuple of low-level features $\boldsymbol{\mu}$ after one step of gradient descent follows

$$\Delta f_h(\boldsymbol{\mu}) = \frac{1}{P} \sum_{\alpha=1}^{n_c} a_{h,\alpha} \left(\hat{N}_1(\boldsymbol{\mu}; \alpha) - \frac{1}{n_c} \sum_{\beta=1}^{n_c} \hat{N}_1(\boldsymbol{\mu}; \beta) \right), \quad (10)$$

where $\mathbf{a}_h = (a_{h,1}, \dots, a_{h,n_c})$ denotes the associated n_c dimensional readout weight. \hat{N}_1 is used to denote the empirical estimate of the occurrences in the first input patch. Hence, by the result of the previous section, the hidden representation becomes insensitive to the exchange of synonymic features for $P \gg P_c$.

This prediction is confirmed empirically in [Fig. 8](#), which shows the sensitivity $S_{1,1}$ of the hidden representation⁴ of shallow fully-connected networks trained in the setting of this section, as a function of the number P of training data for different combinations of the model parameters. The bottom panel, in particular, highlights that the sensitivity is close to 1 for $P \ll P_c$ and close to 0 for $P \gg P_c$. In addition, notice that the collapse of the pre-activations of synonymic tuples onto the same, synonymic invariant value, implies that the rank of the hidden weights matrix tends to v —the vocabulary size of higher-level features. This low-rank structure is typical in the weights of deep networks trained on image classification [34–37]. We discuss the

⁴Here invariance to exchange of level-1 synonyms can already be achieved at the first hidden layer due to the orthogonalization of the s -dimensional patches of the input, which makes them linearly separable.

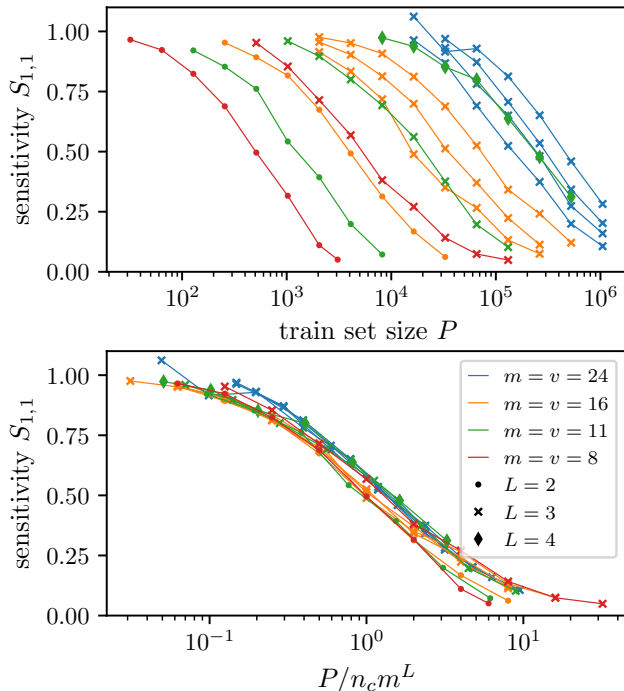


Figure 8: Synonymic sensitivity of the hidden representation vs P for a two-layer fully-connected network trained on the first patch of the inputs of an RHM with $s=2$ and $m=v$, for several values of L , v , and $n_c \leq v$. The top panel shows the bare curves whereas, in the bottom panel, the x-axis is rescaled by $P_c = n_c m^L$. The collapse of the rescaled curves highlights that P_c coincides with the threshold number of training data for building a synonymic invariant representation.

effects of weight sharing or the addition of a clustering step to the learning algorithm [23, 38] in [Supplementary Subsection C.1](#) and [Supplementary Section D](#), respectively.

4 Conclusion

What makes real-world tasks learnable? This question extends from machine learning to brain science [39]. To start thinking quantitatively about it, we introduced the Random Hierarchy Model: a family of tasks that captures the compositional structure of natural data. We showed that neural networks can learn such tasks with a limited training set, by developing a hierarchical representation of the data. Overall, these results rationalize several phenomena associated with deep learning.

First, our finding that for hierarchical tasks, the sample complexity is polynomial in the input dimension (and not exponential) leads to a plausible explanation for the learnability of real-world tasks. Moreover, our results provide a

rule of thumb for estimating the order of magnitude of the sample complexity of benchmark datasets. In the case of CIFAR10 [40], for instance, having 10 classes, taking reasonable values for task parameters such as $m \in [5, 15]$ and $L = 3$, yields $P^* \in [10^3, 3 \times 10^4]$, comparable with the sample complexity of modern architectures (see [Supplementary Fig. 6 in Supplementary Section G](#)).

Secondly, our results quantify the intuition that depth is crucial to building a hierarchical representation that effectively lowers the dimension of the problem, and allows for avoiding the curse of dimensionality. On the one hand, this result gives a foundation to the claim that deep is better than shallow, beyond previous analyses that focused on expressivity [22, 25] rather than learning. On the other hand, our result that the internal representations of trained networks mirror the hierarchical structure of the task explains why these representations become increasingly complex with depth in real-world applications [10, 11].

Furthermore, we provided a characterization of the internal representations based on their sensitivity towards transformations of the low-level features that leave the class label unchanged. This viewpoint complements existing ones that focus instead on the input features that maximize the response of hidden neurons, thus enhancing the interpretability of neural nets. In addition, our approach bypasses several issues of previous characterizations. For example, approaches based on mutual information [13] are ill-defined when the network representations are deterministic functions of the input [14], whereas those based on intrinsic dimension [15, 16] can display counterintuitive results—see [Supplementary Section F](#) for a deeper discussion of the intrinsic dimension and on how it behaves in our framework.

Finally, our study predicts a fundamental relationship between sample complexity, the emergence of invariant representations, and the correlations between low-level features and labels. This prediction can be tested beyond the context of our model, for instance by studying invariance to exchanging synonyms in language modeling tasks.

Looking forward, the Random Hierarchy Model is a suitable candidate for the clarification of other open questions in the theory of deep learning. For instance, a formidable challenge is to obtain a detailed description of the gradient-descent dynamics of deep networks. Indeed, dynamics may be significantly easier to analyze in this model, since quantities characterizing the network success, such as sensitivity to synonyms, can be delineated. Beyond supervised learning, in the Random Hierarchy Model the distribution of input data is itself hierarchical. Thus, this model offers a new handle to study the effect of compositionality on self-supervised learning or probabilistic generative models—extremely powerful techniques whose understanding is still in its infancy.

Methods

RHM implementation

The code implementing the RHM is available online at <https://github.com/pcsl-epfl/hierarchy-learning/blob/master/datasets/hierarchical.py>. The inputs sampled from the RHM are represented as a one-hot encoding of low-level features so that each input consists of s^L pixels and v channels (size $s^L \times v$). The input pixels are whitened over channels, i.e., each pixel has zero mean and unit variance over the channels.

Machine Learning Models

We consider both generic deep neural networks and deep convolutional networks (CNNs) tailored to the structure of the RHM. Generic deep neural networks are made by stacking *fully-connected* layers, i.e., linear transformations of the kind

$$x \in \mathbb{R}^{d_{\text{in}}} \rightarrow W \cdot x + b \in \mathbb{R}^{d_{\text{out}}}, \quad (11)$$

where W is a $d_{\text{out}} \times d_{\text{in}}$ matrix of weights and b a d_{out} sequence of biases. *Convolutional* layers, instead, act on image-like inputs that have a spatial dimension d and c_{in} channels and compute the convolution of the input with a filter of spatial size f . This operation is equivalent to applying the linear transformation of [Eq. \(11\)](#) to input patches of spatial size f , i.e., groups of f adjacent pixels (dimension $d_{\text{in}} = (f \times c_{\text{in}})$). The output has an image-like structure analogous to that of the input, with spatial dimension depending on how many patches are considered. In the *nonoverlapping patches* case, for instance, the spatial dimension of the output is d/f .

For all layers but the last, the linear transformation is followed by an element-wise nonlinear activation function σ . We resort to the popular Rectified Linear Unit (ReLU) $\sigma(x) = \max(0, x)$. The output dimension is always fixed to the number of classes n_c . The input dimension is the same as the input data: spatial dimension s^L and v channels, flattened into a single $s^L \times v$ sequence when using a fully-connected layer. The dimensionalities of the other *hidden* layers are kept constant throughout the network and set to a multiple of v^s . Increasing this number further does not affect any of the results presented in the paper.

To tailor deep CNNs to the structure of the RHM, we set $f = s$ so that, in the nonoverlapping patches setting, each convolutional filter acts on a group of s low-level features that correspond to the same higher-level feature. Since the spatial dimensionality of the input is s^L and each layer reduces it by s , the number of nonlinear layers in a tailored CNN is fixed to the depth of the RHM L , so that the network depth is $L + 1$. Fully-connected networks, instead,

can have any depth. The code for the implementation of both architectures is available at <https://github.com/pcsl-epfl/hierarchy-learning/blob/master/models>.

Training Procedure

Training is performed within the PyTorch deep learning framework [41]. Neural networks are trained on P training points sampled uniformly at random from the RHM data, using stochastic gradient descent (SGD) on the cross-entropy loss. The batch size is 128 for $P \geq 128$ and P otherwise, the learning rate is initialised to 10^{-1} and follows a cosine annealing schedule which reduces it to 10^{-2} over 100 epochs. Training stops when the training loss reaches 10^{-3} . The corresponding code is available at <https://github.com/pcsl-epfl/hierarchy-learning/blob/master>

The performance of the trained models is measured as the classification error on a test set. The size of the test set is set to $\min(P_{\max} - P, 20'000)$. Synonymic sensitivity, as defined in Eq. (7), is measured on a test set of size $\min(P_{\max} - P, 1'000)$. Reported results for a given value of RHM parameters are averaged over 10 jointly different instances of the RHM and network initialization.

Acknowledgements

We thank Antonio Sclocchi for fruitful discussions and helpful feedback on the manuscript.

Author contributions

F.C. and M.W. led the theory development, L.P. led experimental design and execution. M.W. introduced the model and directed the research. All authors contributed to discussions. The manuscript was primarily written by F.C., L.P., and M.W., with constructive feedback and revisions provided by U.M.T. and A.F.

References

1. Voulodimos, A., Doulamis, N., Doulamis, A. & Protopapadakis, E. Deep Learning for Computer Vision: A Brief Review. *Computational Intelligence and Neuroscience*, 1–13 (2018).
2. Silver, D. *et al.* Mastering the game of go without human knowledge. *Nature* **550**, 354–359 (2017).
3. Bach, F. Breaking the curse of dimensionality with convex neural networks. *The Journal of Machine Learning Research* **18**, 629–681 (2017).
4. Luxburg, U. v. & Bousquet, O. Distance-based classification with Lipschitz functions. *The Journal of Machine Learning Research* **5**, 669–695 (2004).
5. Deng, J. *et al.* Imagenet: A large-scale hierarchical image database in 2009 IEEE conference on computer vision and pattern recognition (2009), 248–255.
6. Pope, P., Zhu, C., Abdelkader, A., Goldblum, M. & Goldstein, T. *The Intrinsic Dimension of Images and Its Impact on Learning in International Conference on Learning Representations* (2021).
7. LeCun, Y., Bengio, Y. & Hinton, G. Deep learning. *Nature* **521**, 436 (2015).
8. Van Essen, D. C. & Maunsell, J. H. Hierarchical organization and functional streams in the visual cortex. *Trends in neurosciences* **6**, 370–375 (1983).
9. Grill-Spector, K. & Malach, R. The human visual cortex. *Annu. Rev. Neurosci.* **27**, 649–677 (2004).
10. Zeiler, M. D. & Fergus, R. *Visualizing and Understanding Convolutional Networks in Computer Vision – ECCV 2014* (2014), 818–833.
11. Doimo, D., Glielmo, A., Ansuini, A. & Laio, A. Hierarchical nucleation in deep neural networks. *Advances in Neural Information Processing Systems* **33**, 7526–7536 (2020).
12. Bruna, J. & Mallat, S. Invariant scattering convolution networks. *IEEE transactions on pattern analysis and machine intelligence* **35**, 1872–1886 (2013).
13. Shwartz-Ziv, R. & Tishby, N. Opening the Black Box of Deep Neural Networks via Information. *Preprint at <http://arxiv.org/abs/1703.00810>*. (2017).
14. Saxe, A. M. *et al.* On the information bottleneck theory of deep learning. *Journal of Statistical Mechanics: Theory and Experiment* **2019**, 124020 (2019).
15. Ansuini, A., Laio, A., Macke, J. H. & Zoccolan, D. Intrinsic dimension of data representations in deep neural networks. *Advances in Neural Information Processing Systems* **32**, 6111–6122 (2019).
16. Recanatesi, S. *et al.* Dimensionality compression and expansion in Deep Neural Networks. *Preprint at <http://arxiv.org/abs/1906.00443>*. (2019).
17. Petrini, L., Favero, A., Geiger, M. & Wyart, M. Relative stability toward diffeomorphisms indicates performance in deep nets. *Advances in Neural Information Processing Systems* **34**, 8727–8739 (2021).
18. Tomasini, U. M., Petrini, L., Cagnetta, F. & Wyart, M. How deep convolutional neural networks lose spatial information with training. *Machine Learning: Science and Technology* **4**, 045026 (2023).
19. Patel, A. B., Nguyen, T. & Baraniuk, R. G. A probabilistic theory of deep learning. *Preprint at <https://arxiv.org/abs/1504.00641>*. (2015).

20. Mossel, E. Deep Learning and Hierarchical Generative Models. *Preprint at <http://arxiv.org/abs/1612.09057>*. (2018).
21. Mhaskar, H., Liao, Q. & Poggio, T. When and Why Are Deep Networks Better Than Shallow Ones? *Proceedings of the AAAI Conference on Artificial Intelligence* **31** (2017).
22. Poggio, T., Mhaskar, H., Rosasco, L., Miranda, B. & Liao, Q. Why and when can deep-but not shallow-networks avoid the curse of dimensionality: a review. *International Journal of Automation and Computing* **14**, 503–519 (2017).
23. Malach, E. & Shalev-Shwartz, S. A Provably Correct Algorithm for Deep Learning that Actually Works. *Preprint at <http://arxiv.org/abs/1803.09522>*. (2018).
24. Zazo, J., Tolooshams, B., Ba, D. & Paulson, H. J. A. Convolutional Dictionary Learning in Hierarchical Networks. *IEEE 8th International Workshop on Computational Advances in Multi-Sensor Adaptive Processing*, 131–135 (2019).
25. Schmidt-Hieber, J. Nonparametric regression using deep neural networks with ReLU activation function. *The Annals of Statistics* **48**, 1875–1897 (2020).
26. Cagnetta, F., Favero, A. & Wyart, M. *What can be learnt with wide convolutional neural networks?* in *International Conference on Machine Learning* (2023), 3347–3379.
27. Saxe, A. M., McClelland, J. L. & Ganguli, S. Exact solutions to the nonlinear dynamics of learning in deep linear neural networks. *International Conference on Learning Representations* (2014).
28. Mézard, M. Mean-field message-passing equations in the Hopfield model and its generalizations. *Physical Review E* **95**, 022117 (2017).
29. Ingrosso, A. & Goldt, S. Data-driven emergence of convolutional structure in neural networks. *Proceedings of the National Academy of Sciences* **119** (2022).
30. Feng, Y. & Tu, Y. The inverse variance–flatness relation in stochastic gradient descent is critical for finding flat minima. *Proceedings of the National Academy of Sciences* **118** (2021).
31. Rozenberg, G. & Salomaa, A. *Handbook of Formal Languages* (Springer, Jan. 1997).
32. Damian, A., Lee, J. & Soltanolkotabi, M. Neural Networks can Learn Representations with Gradient Descent. *Proceedings of Thirty-Fifth Conference on Learning Theory* **178**, 5413–5452 (2022).
33. Ba, J. *et al.* High-dimensional Asymptotics of Feature Learning: How One Gradient Step Improves the Representation. *Advances in Neural Information Processing Systems* **35**, 37932–37946 (2022).
34. Denil, M., Shakibi, B., Dinh, L., Ranzato, M. A. & de Freitas, N. *Predicting Parameters in Deep Learning in Advances in Neural Information Processing Systems* **26** (2013).
35. Denton, E. L., Zaremba, W., Bruna, J., LeCun, Y. & Fergus, R. *Exploiting Linear Structure Within Convolutional Networks for Efficient Evaluation in Advances in Neural Information Processing Systems* **27** (2014).
36. Yu, X., Liu, T., Wang, X. & Tao, D. On Compressing Deep Models by Low Rank and Sparse Decomposition. *2017 IEEE Conference on Computer Vision and Pattern Recognition (CVPR)*, 67–76 (2017).
37. Guth, F., Ménard, B., Rochette, G. & Mallat, S. A Rainbow in Deep Network Black Boxes. *Preprint at <http://arxiv.org/abs/2305.18512>*. (2023).
38. Malach, E. & Shalev-Shwartz, S. The implications of local correlation on learning some deep functions. *Advances in Neural Information Processing Systems* **33**, 1322–1332 (2020).
39. Kruger, N. *et al.* Deep hierarchies in the primate visual cortex: What can we learn for computer vision? *IEEE transactions on pattern analysis and machine intelligence* **35**, 1847–1871 (2012).
40. Krizhevsky, A. Learning multiple layers of features from tiny images. *Preprint at <https://www.cs.toronto.edu/~kriz/learning-features-2009-TR.pdf>*. (2009).
41. Paszke, A. *et al.* PyTorch: An Imperative Style, High-Performance Deep Learning Library. *Advances in Neural Information Processing Systems* **32** (2019).

Supplementary Information for “How Deep Neural Networks Learn Compositional Data: The Random Hierarchy Model”

A Statistics of The Composition Rules

In this section, we consider a single composition rule, that is the assignment of m s -tuples of low-level features to each of the v high-level features. In the RHM these rules are chosen uniformly at random over all the possible rules, thus their statistics are crucial in determining the correlations between the input features and the class label.

A.1 Statistics of a single rule

For each rule, we call $N_i(\mu_1; \mu_2)$ the number of occurrences of the low-level feature μ_1 in position i of the s -tuples generated by the higher-level feature μ_2 . The probability of $N_i(\mu_1; \mu_2)$ is that of the number of successes when drawing m (number of s -tuples associated with the high-level feature μ_2) times without replacement from a pool of v^s (total number of s -tuples with vocabulary size v) objects where only v^{s-1} satisfy a certain condition (number of s -tuples displaying feature μ_1 in position i):

$$\Pr \{N_i(\mu_0; \mu_1) = k\} = \binom{v^{s-1}}{k} \binom{v^s - v^{s-1}}{m - k} / \binom{v^s}{m}, \quad (1)$$

which is a Hypergeometric distribution $\text{Hg}_{v^s, v^{s-1}, m}$, with mean

$$\langle N \rangle = m \frac{v^{s-1}}{v^s} = \frac{m}{v}, \quad (2)$$

and variance

$$\sigma_N^2 := \langle (N - \langle N \rangle)^2 \rangle = m \frac{v^{s-1}}{v^s} \frac{v^s - v^{s-1}}{v^s} \frac{v^s - m}{v^s - 1} = \frac{m}{v} \frac{v - 1}{v} \frac{v^s - m}{v^s - 1} \xrightarrow{m \gg 1} \frac{m}{v}, \quad (3)$$

independently of the position i and the specific low- and high-level features. Notice that, since $m \leq v^{s-1}$ with s fixed, large m implies also large v .

A.2 Joint statistics of a single rule

Shared high-level feature. For a fixed high-level feature μ_2 , the joint probability of the occurrences of two different low-level features μ_1 and ν_1 is a multivariate Hypergeometric distribution,

$$\Pr \{N_i(\mu_1; \mu_2) = k; N_i(\nu_1; \mu_2) = l\} = \binom{v^{s-1}}{k} \binom{v^{s-1}}{l} \binom{v^s - 2v^{s-1}}{m - k - l} / \binom{v^s}{m}, \quad (4)$$

giving the following covariance,

$$c_N := \langle (N_i(\mu_1; \mu_2) - \langle N \rangle) (N_i(\nu_1; \mu_2) - \langle N \rangle) \rangle = -\frac{m}{v^2} \frac{v^s - m}{v^s - 1} \xrightarrow{m \gg 1} -\left(\frac{m}{v}\right)^2 \frac{1}{m}. \quad (5)$$

The covariance can also be obtained via the constraint $\sum_{\mu_1} N_i(\mu_1; \mu_2) = m$. For any finite sequence of identically distributed random variables X_μ with a constraint on the sum $\sum_{\mu} X_\mu = m$,

$$\begin{aligned} \sum_{\mu=1}^v X_\mu = m &\Rightarrow \sum_{\mu=1}^v (X_\mu - \langle X_\mu \rangle) = 0 \Rightarrow \\ (X_\nu - \langle X_\nu \rangle) \sum_{\mu=1}^v (X_\mu - \langle X_\mu \rangle) &= 0 \Rightarrow \sum_{\mu=1}^v \langle (X_\nu - \langle X_\nu \rangle) (X_\mu - \langle X_\mu \rangle) \rangle = 0 \Rightarrow \\ \text{Var} [X_\mu] + (v - 1) \text{Cov} [X_\mu, X_\nu] &= 0. \end{aligned} \quad (6)$$

In the last line, we used the identically distributed variables hypothesis to replace the sum over $\mu \neq \nu$ with the factor $(v - 1)$. Therefore,

$$c_N = \text{Cov} [N_i(\mu_1; \mu_2), N_i(\nu_1; \mu_2)] = -\frac{\text{Var} [N_i(\mu_1; \mu_2)]}{v - 1} = -\frac{\sigma_N^2}{v - 1}. \quad (7)$$

Shared low-level feature. The joint probability of the occurrences of the same low-level feature μ_1 starting from different high-level features $\mu_2 \neq \nu_2$ can be written as follows,

$$\Pr \{N(\mu_1; \mu_2) = k; N(\mu_1; \nu_2) = l\} = \Pr \{N(\mu_1; \mu_2) = k | N(\mu_1; \nu_2) = l\} \times \Pr \{N(\mu_1; \nu_2) = l\} \quad (8)$$

$$= \text{Hg}_{v^s - m, v^{s-1} - l, m}(k) \times \text{Hg}_{v^s, v^{s-1}, m}(l), \quad (9)$$

resulting in the following ‘inter-feature’ covariance,

$$c_{if} := \text{Cov} [N_i(\mu_1; \mu_2), N_i(\mu_1; \nu_2)] = - \left(\frac{m}{v}\right)^2 \frac{v-1}{v^s-1}. \quad (10)$$

No shared features. Finally, by multiplying both sides of $\sum_{\mu_1} N(\mu_1; \mu_2) = m$ with $N(\nu_1; \nu_2)$ and averaging, we get

$$c_g := \text{Cov} [N_i(\mu_1; \mu_2), N_i(\nu_1; \nu_2)] = - \frac{\text{Cov} [N_i(\mu_1; \mu_2), N_i(\mu_1; \nu_2)]}{v-1} = \left(\frac{m}{v}\right)^2 \frac{1}{v^s-1}. \quad (11)$$

B Emergence of input-output correlations (P_c)

As discussed in the main text, the Random Hierarchy Model presents a characteristic sample size P_c corresponding to the emergence of the input-output correlations. This sample size predicts the sample complexity of deep CNNs, as we also discuss in the main text. In this appendix, we prove that

$$P_c \xrightarrow{n_c, m \rightarrow \infty} n_c m^L. \quad (12)$$

B.1 Estimating the Signal

The correlations between input features and the class label can be quantified via the conditional probability (over realizations of the RHM) of a data point belonging to class α conditioned on displaying the s -tuple $\boldsymbol{\mu}$ in the j -th input patch,

$$f_j(\alpha | \boldsymbol{\mu}) := \Pr \{ \mathbf{x} \in \alpha | \mathbf{x}_j = \boldsymbol{\mu} \}, \quad (13)$$

where the notation $\mathbf{x}_j = \boldsymbol{\mu}$ means that the elements of the patch \mathbf{x}_j encode the tuple of features $\boldsymbol{\mu}$. We say that the low-level features are correlated with the output if

$$f_j(\alpha | \boldsymbol{\mu}) \neq \frac{1}{n_c}, \quad (14)$$

and define a ‘signal’ as the difference $f_j(\alpha | \boldsymbol{\mu}) - n_c^{-1}$. In the following, we compute the statistics of the signal over realizations of the RHM.

Occurrence of low-level features. Let us begin by defining the joint occurrences of a class label α and a low-level feature μ_1 in a given position of the input. Using the tree representation of the model, we will identify an input position with a set of L indices $i_\ell = 1, \dots, s$, each indicating which branch to follow when descending from the root (class label) to a given leaf (low-level feature). These joint occurrences can be computed by combining the occurrences of the single rules introduced in [Supplementary Section A](#). With $L = 2$, for instance,

$$N_{i_1 i_2}^{(1 \rightarrow 2)}(\mu_1; \alpha) = \sum_{\mu_2=1}^v \left(m^{s-1} N_{i_1}^{(1)}(\mu_1; \mu_2) \right) \times N_{i_2}^{(2)}(\mu_2; \alpha), \quad (15)$$

where:

- i)* $N_{i_2}^{(2)}(\mu_2; \alpha)$ ⁵ counts the occurrences of μ_2 in position i_2 of the level-2 representations of α , i.e. the s -tuples generated from α according to the second-layer composition rule;

⁵We are using the superscript (ℓ) to differentiate the occurrences of the different composition rules.

- ii) $N_{i_1}^{(1)}(\mu_1; \mu_2)$ counts the occurrences of μ_1 in position i_1 of the level-1 representations of μ_2 , i.e. s -tuples generated by μ_2 according to the composition rule of the first layer;
- iii) the factor m^{s-1} counts the descendants of the remaining $s-1$ elements of the level-2 representation (m descendants per element);
- iv) the sum over μ_2 counts all the possible paths of features that lead to μ_1 from α across 2 generations.

The generalization of Eq. (15) is immediate once one takes into account that the multiplicity factor accounting for the descendants of the remaining positions at the ℓ -th generation is equal to $m^{s^{\ell-1}}/m$ ($s^{\ell-1}$ is the size of the representation at the previous level). Hence, the overall multiplicity factor after L generations is

$$1 \times \frac{m^s}{m} \times \frac{m^{s^2}}{m} \times \cdots \times \frac{m^{s^{L-1}}}{m} = m^{\frac{s^L-1}{s-1}-L}, \quad (16)$$

so that the number of occurrences of feature μ_1 in position $i_1 \dots i_L$ of the inputs belonging to class α is

$$N_{i_1 \rightarrow L}^{(1 \rightarrow L)}(\mu_1; \alpha) = m^{\frac{s^L-1}{s-1}-L} \sum_{\mu_2, \dots, \mu_L=1}^v N_{i_1}^{(1)}(\mu_1; \mu_2) \times \cdots \times N_{i_L}^{(L)}(\mu_L; \alpha), \quad (17)$$

where we used $i_1 \rightarrow L$ as a shorthand notation for the tuple of indices i_1, i_2, \dots, i_L .

The same construction allows us to compute the number of occurrences of up to $s-1$ features within the s -dimensional patch of the input corresponding to the path $i_2 \rightarrow L$. The number of occurrences of a whole s -tuple, instead, follows a slightly different rule, since there is only one level-2 feature μ_2 which generates the whole s -tuple of level-1 features $\mu_1 = (\mu_{1,1}, \dots, \mu_{1,s})$ —we call this feature $g_1(\mu_1)$, with g_1 denoting the first-layer composition rule. As a result, the sum over μ_2 in the right-hand side of Eq. (17) disappears and we are left with

$$N_{i_2 \rightarrow L}^{(1 \rightarrow L)}(\mu_1; \alpha) = m^{\frac{s^L-1}{s-1}-L} \sum_{\mu_3, \dots, \mu_L=1}^v N_{i_2}^{(2)}(g_1(\mu_1); \mu_3) \times \cdots \times N_{i_L}^{(L)}(\mu_L; \alpha). \quad (18)$$

Coincidentally, Eq. (18) shows that the joint occurrences of a s -tuple of low-level features μ_1 depend on the level-2 feature corresponding to μ_1 . Hence, $N_{i_2 \rightarrow L}^{(1 \rightarrow L)}(\mu_1; \alpha)$ is invariant for the exchange of μ_1 with one of its synonyms, i.e. level-1 tuples ν_1 corresponding to the same level-2 feature.

Class probability conditioned on low-level observations. We can turn these numbers into probabilities by normalizing them appropriately. Upon dividing by the total occurrences of a low-level feature μ_1 independently of the class, for instance, we obtain the conditional probability of the class of a given input, conditioned on the feature in position $i_1 \dots i_L$ being μ_1 .

$$f_{i_1 \rightarrow L}^{(1 \rightarrow L)}(\alpha | \mu_1) := \frac{N_{i_1 \rightarrow L}^{(1 \rightarrow L)}(\mu_1; \alpha)}{\sum_{\alpha'=1}^{n_c} N_{i_1 \rightarrow L}^{(1 \rightarrow L)}(\mu_1; \alpha')} = \frac{\sum_{\mu_2, \dots, \mu_L=1}^v N_{i_1}^{(1)}(\mu_1; \mu_2) \times \cdots \times N_{i_L}^{(L)}(\mu_L; \alpha)}{\sum_{\mu_2, \dots, \mu_L=1}^v \sum_{\mu_{L+1}=1}^{n_c} N_{i_1}^{(1)}(\mu_1; \mu_2) \times \cdots \times N_{i_L}^{(L)}(\mu_L; \mu_{L+1})}. \quad (19)$$

Let us also introduce, for convenience, the numerator and denominator of the right-hand side of Eq. (19).

$$U_{i_1 \rightarrow L}^{(1 \rightarrow L)}(\mu_1; \alpha) = \sum_{\mu_2, \dots, \mu_L=1}^v N_{i_1}^{(1)}(\mu_1; \mu_2) \times \cdots \times N_{i_L}^{(L)}(\mu_L; \alpha); \quad D_{i_1 \rightarrow L}^{(1 \rightarrow L)}(\mu_1) = \sum_{\alpha=1}^{n_c} U_{i_1 \rightarrow L}^{(1 \rightarrow L)}(\mu_1; \alpha). \quad (20)$$

B.1.1 Statistics of the numerator U

We now determine the first and second moments of the numerator of $f_{i_1 \rightarrow L}^{(1 \rightarrow L)}(\mu_1; \alpha)$. Let us first recall the definition for clarity,

$$U_{i_1 \rightarrow L}^{(1 \rightarrow L)}(\mu_1; \alpha) = \sum_{\mu_2, \dots, \mu_L=1}^v N_{i_1}^{(1)}(\mu_1; \mu_2) \times \cdots \times N_{i_L}^{(L)}(\mu_L; \alpha) \quad (21)$$

Level 1 $L=1$. For $L=1$, U is simply the occurrence of a single production rule $N_i(\mu_1; \alpha)$,

$$\langle U^{(1)} \rangle = \frac{m}{v}; \quad (22)$$

$$\sigma_{U^{(1)}}^2 := \text{Var} [U^{(1)}] = \frac{m}{v} \frac{v-1}{v} \frac{v^s - m}{v^s - 1} \xrightarrow{v \gg 1} \frac{m}{v}; \quad (23)$$

$$c_{U^{(1)}} := \text{Cov} [U^{(1)}(\mu_1; \alpha), U^{(1)}(\nu_1; \alpha)] = -\frac{\text{Var} [U^{(1)}]}{(v-1)} = -\left(\frac{m}{v}\right)^2 \frac{v^s - m}{v^s - 1} \frac{1}{m} \xrightarrow{v \gg 1} \left(\frac{m}{v}\right)^2 \frac{1}{m}; \quad (24)$$

where the relationship between variance and covariance is due to the constraint on the sum of $U^{(1)}$ over μ_1 , see Eq. (6).

Level 2 $L=2$. For $L=2$,

$$U_{i_1 \rightarrow 2}^{(1 \rightarrow 2)}(\mu_1; \alpha) = \sum_{\mu_2=1}^v N_{i_1}^{(1)}(\mu_1; \mu_2) \times N_{i_2}^{(2)}(\mu_2; \alpha) = \sum_{\mu_2=1}^v N_{i_1}^{(1)}(\mu_1; \mu_2) U_{i_2}^{(2)}(\mu_2; \alpha). \quad (25)$$

Therefore,

$$\langle U^{(1 \rightarrow 2)} \rangle = v \left(\frac{m}{v}\right) \times \langle U^{(1)} \rangle = v \left(\frac{m}{v}\right)^2; \quad (26)$$

$$\begin{aligned} \sigma_{U^{(2)}}^2 := \text{Var} [U^{(1 \rightarrow 2)}] &= \sum_{\mu_2, \nu_2=1}^v \left(\langle N^{(1)}(\mu_1; \mu_2) N^{(1)}(\mu_1; \nu_2) \rangle \langle U^{(2)}(\mu_2; \alpha) U^{(2)}(\nu_2; \alpha) \rangle - \langle N \rangle^2 \langle U^{(1)} \rangle^2 \right) \\ &= \sum_{\mu_2, \nu_2=\mu_2} \dots + \sum_{\mu_2} \sum_{\nu_2 \neq \mu_2} \dots \\ &= v \left(\sigma_N^2 \sigma_{U^{(1)}}^2 + \sigma_N^2 \langle U^{(1)} \rangle^2 + \sigma_{U^{(1)}}^2 \langle N \rangle^2 \right) + v(v-1) \left(c_{if} c_{U^{(1)}} + c_{if} \langle U^{(1)} \rangle^2 + c_{U^{(1)}} \langle N \rangle^2 \right) \\ &= v \left(\sigma_N^2 \sigma_{U^{(1)}}^2 + (v-1) c_{if} c_{U^{(1)}} \right) + v \langle U^{(1)} \rangle^2 \left(\sigma_N^2 + (v-1) c_{if} \right) + v \langle N \rangle^2 \left(\sigma_{U^{(1)}}^2 + (v-1) c_{U^{(1)}} \right) \\ &= v \sigma_{U^{(1)}}^2 \left(\sigma_N^2 - c_{if} \right) + v \langle U^{(1)} \rangle^2 \left(\sigma_N^2 + (v-1) c_{if} \right), \end{aligned} \quad (27)$$

$$c_{U^{(2)}} = -\frac{\sigma_{U^{(2)}}^2}{(v-1)} \quad (28)$$

Level L. In general,

$$U_{i_1 \rightarrow L}^{(1 \rightarrow L)}(\mu_1; \alpha) = \sum_{\mu_2=1}^v N_{i_1}^{(1)}(\mu_1; \mu_2) U_{i_2 \rightarrow L}^{(2 \rightarrow L)}(\mu_2; \alpha). \quad (29)$$

Therefore,

$$\langle U^{(L)} \rangle = v \left(\frac{m}{v}\right) \times \langle U^{(L-1)} \rangle = v^{L-1} \left(\frac{m}{v}\right)^L; \quad (30)$$

$$\begin{aligned} \sigma_{U^{(L)}}^2 &= \sum_{\mu_2, \nu_2=1}^v \left(\langle N^{(1)}(\mu_1; \mu_2) N^{(1)}(\mu_1; \nu_2) \rangle \langle U^{(2 \rightarrow L)}(\mu_2; \alpha) U^{(2 \rightarrow L)}(\nu_2; \alpha) \rangle - \langle N \rangle^2 \langle U^{(1 \rightarrow (L-1))} \rangle^2 \right) \\ &= \sum_{\mu_2, \nu_2=\mu_2} \dots + \sum_{\mu_2} \sum_{\nu_2 \neq \mu_2} \dots \\ &= v \left(\sigma_N^2 \sigma_{U^{(L-1)}}^2 + \sigma_N^2 \langle U^{(L-1)} \rangle^2 + \sigma_{U^{(L-1)}}^2 \langle N \rangle^2 \right) + v(v-1) \left(\sigma_{if}^2 c_{U^{(L-1)}} + c_{if} \langle U^{(L-1)} \rangle^2 + c_{U^{(L-1)}} \langle N \rangle^2 \right) \\ &= v \sigma_{U^{(L-1)}}^2 \left(\sigma_N^2 - c_{if} \right) + v \langle U^{(L-1)} \rangle^2 \left(\sigma_N^2 + (v-1) c_{if} \right), \end{aligned} \quad (31)$$

$$c_{U^{(L)}} = -\frac{\sigma_{U^{(L)}}^2}{(v-1)} \quad (32)$$

Concentration for large m . In the large multiplicity limit $m \gg 1$, the U 's concentrate around their mean value. Due to $m \leq v^{s-1}$, large m implies large v , thus we can proceed by setting $m = qv^{s-1}$, with $q \in (0, 1]$ ⁶ and studying the $v \gg 1$ limit. From Eq. (30),

$$\langle U^{(L)} \rangle = q^L v^{L(s-1)-1}. \quad (33)$$

In addition,

$$\sigma_N^2 \xrightarrow{v \gg 1} \frac{m}{v} = qv^{(s-1)-1}, \quad c_{if} \xrightarrow{v \gg 1} -\left(\frac{m}{v}\right)^2 \frac{1}{v^{s-1}} = -q^2 v^{(s-1)-2}, \quad (34)$$

so that

$$\begin{aligned} \sigma_{U^{(L)}}^2 &= v \sigma_{U^{(L-1)}}^2 (\sigma_N^2 - \sigma_{if}^2) + v \langle U^{(L-1)} \rangle^2 (\sigma_N^2 + (v-1)\sigma_{if}^2) \\ &\xrightarrow{v \gg 1} \sigma_{U^{(L-1)}}^2 qv^{(s-1)} + \sigma_{U^{(L-1)}}^2 q^2 v^{(s-1)-1} + q^{2L-1} (1-q) v^{(2L-1)(s-1)-2} \end{aligned} \quad (35)$$

The second of the three terms is always subleading with respect to the first, so we can discard it for now. It remains to compare the first and the third terms. For $L=2$, since $\sigma_{U^{(1)}}^2 = \sigma_N^2$, the first term depends on v as $v^{2(s-1)-1}$, whereas the third is proportional to $v^{3(s-1)-2}$. For $L \geq 3$ the dominant scaling is that of the third term only: for $L=3$ it can be shown by simply plugging the $L=2$ result into the recursion, and for larger L it follows from the fact that replacing $\sigma_{U^{(L-1)}}^2$ in the first term with the third term of the previous step always yields a subdominant contribution. Therefore,

$$\sigma_{U^{(L)}}^2 \xrightarrow{v \gg 1} \begin{cases} q^2 v^{2(s-1)-1} + q^3 (1-q) v^{3(s-1)-2}, & \text{for } L=2, \\ q^{2L-1} (1-q) v^{(2L-1)(s-1)-2}, & \text{for } L \geq 3. \end{cases} \quad (36)$$

Upon dividing the variance by the squared mean we get

$$\frac{\sigma_{U^{(L)}}^2}{\langle U^{(L)} \rangle^2} \xrightarrow{v \gg 1} \begin{cases} \frac{1}{q^2} \frac{1}{v^{2(s-1)-1}} + \frac{1-q}{q} \frac{1}{v^{(s-1)}}, & \text{for } L=2, \\ \frac{1-q}{q} \frac{1}{v^{(s-1)}}, & \text{for } L \geq 3, \end{cases} \quad (37)$$

whose convergence to 0 guarantees the concentration of the U 's around the average over all instances of the RHM.

B.1.2 Statistics of the denominator D

Here we compute the first and second moments of the denominator of $f_{i_1 \rightarrow L}^{(1 \rightarrow L)}(\mu_1; \alpha)$,

$$D_{i_1 \rightarrow L}^{(1 \rightarrow L)}(\mu_1) = \sum_{\mu_2, \dots, \mu_L=1}^v \sum_{\mu_{L+1}=1}^{n_c} N_{i_1}^{(1)}(\mu_1; \mu_2) \times \dots \times N_{i_L}^{(L)}(\mu_L; \mu_{L+1}) \quad (38)$$

Level 1 $L=1$. For $L=1$, D is simply the sum over classes of the occurrences of a single production rule, $D^{(1)} = \sum_{\alpha} N_i(\mu_1; \alpha)$,

$$\langle D^{(1)} \rangle = n_c \frac{m}{v}; \quad (39)$$

$$\begin{aligned} \sigma_{D^{(1)}}^2 &:= \text{Var} [D^{(1)}] = n_c \sigma_N^2 + n_c (n_c - 1) c_{if} = n_c \left(\frac{m}{v}\right)^2 \frac{v-1}{v^s-1} \left(\frac{v^s}{m} - n_c\right) \\ &\xrightarrow{v \gg 1} n_c \left(\frac{m}{v}\right)^2 \left(\frac{v}{m} - \frac{n_c}{v^{s-1}}\right); \end{aligned} \quad (40)$$

$$c_{D^{(1)}} := \text{Cov} [D^{(1)}(\mu_1), D^{(1)}(\nu_0)] = -\frac{\text{Var} [D^{(1)}]}{(v-1)} = n_c c_N + n_c (n_c - 1) c_g, \quad (41)$$

where, in the last line, we used the identities $\sigma_N^2 + (v-1)c_N = 0$ from Eq. (5) and $c_{if} + (v-1)c_g = 0$ from Eq. (11).

⁶The minimum m is 1, which corresponds to $q = v^{1-s}$, but actually there is no stochasticity in the U 's and D 's in that case. Thus the minimal q is actually $2v^{1-s}$.

Level 2 $L=2$. For $L=2$,

$$D_{i_1 \rightarrow 2}^{(1 \rightarrow 2)}(\mu_1) = \sum_{\mu_2}^v \sum_{\mu_3=1}^{n_c} N_{i_1}^{(1)}(\mu_1; \mu_2) \times N_{i_2}^{(2)}(\mu_2; \mu_3) = \sum_{\mu_2=1}^v N_{i_1}^{(1)}(\mu_1; \mu_2) D_{i_2}^{(2)}(\mu_2). \quad (42)$$

Therefore,

$$\langle D^{(1 \rightarrow 2)} \rangle = v \left(\frac{m}{v} \right) \times \langle D^{(1)} \rangle = \frac{n_c}{v} m^2; \quad (43)$$

$$\begin{aligned} \sigma_{D^{(2)}}^2 := \text{Var} \left[D^{(1 \rightarrow 2)} \right] &= \sum_{\mu_2, \nu_1=1}^v \left(\langle N^{(1)}(\mu_1; \mu_2) N^{(1)}(\mu_1; \nu_1) \rangle \langle D^{(2)}(\mu_2) D^{(2)}(\nu_1) \rangle - \langle N \rangle^2 \langle D^{(1)} \rangle^2 \right) \\ &= \sum_{\mu_2, \nu_1=\mu_2} \dots + \sum_{\mu_2} \sum_{\nu_1 \neq \mu_2} \dots \\ &= v \left(\sigma_N^2 \sigma_{D^{(1)}}^2 + \sigma_N^2 \langle D^{(1)} \rangle^2 + \sigma_{D^{(1)}}^2 \langle N \rangle^2 \right) + v(v-1) \left(c_{if} c_{D^{(1)}} + c_{if} \langle D^{(1)} \rangle^2 + c_{D^{(1)}} \langle N \rangle^2 \right) \\ &= v \left(\sigma_N^2 \sigma_{D^{(1)}}^2 + (v-1) c_{if} c_{D^{(1)}} \right) + v \langle D^{(1)} \rangle^2 \left(\sigma_N^2 + (v-1) c_{if} \right) + v \langle N \rangle^2 \left(\sigma_{D^{(1)}}^2 + (v-1) c_{D^{(1)}} \right) \\ &= v \sigma_{D^{(1)}}^2 \left(\sigma_N^2 - c_{if} \right) + v \langle D^{(1)} \rangle^2 \left(\sigma_N^2 + (v-1) c_{if} \right), \end{aligned} \quad (44)$$

$$c_{D^{(2)}} = -\frac{\sigma_{D^{(2)}}^2}{(v-1)}. \quad (45)$$

Level L. In general,

$$D_{i_1 \rightarrow L}^{(1 \rightarrow L)}(\mu_1) = \sum_{\mu_2=1}^v N_{i_1}^{(1)}(\mu_1; \mu_2) D_{i_2 \rightarrow L}^{(2 \rightarrow L)}(\mu_2). \quad (46)$$

Therefore,

$$\langle D^{(L)} \rangle = v \left(\frac{m}{v} \right) \times \langle D^{(L-1)} \rangle = \frac{n_c}{v} m^L; \quad (47)$$

$$\begin{aligned} \sigma_{D^{(L)}}^2 &= \sum_{\mu_2, \nu_1=1}^v \left(\langle N^{(1)}(\mu_1; \mu_2) N^{(1)}(\mu_1; \nu_1) \rangle \langle D^{(2 \rightarrow L)}(\mu_2; \alpha) D^{(2 \rightarrow L)}(\nu_1; \alpha) \rangle - \langle N \rangle^2 \langle D^{(1 \rightarrow (L-1))} \rangle^2 \right) \\ &= \sum_{\mu_2, \nu_1=\mu_2} \dots + \sum_{\mu_2} \sum_{\nu_1 \neq \mu_2} \dots \\ &= v \left(\sigma_N^2 \sigma_{D^{(L-1)}}^2 + \sigma_N^2 \langle D^{(L-1)} \rangle^2 + \sigma_{D^{(L-1)}}^2 \langle N \rangle^2 \right) + v(v-1) \left(c_{if} c_{D^{(L-1)}} + c_{if} \langle D^{(L-1)} \rangle^2 + c_{D^{(L-1)}} \langle N \rangle^2 \right) \\ &= v \sigma_{D^{(L-1)}}^2 \left(\sigma_N^2 - c_{if} \right) + v \langle D^{(L-1)} \rangle^2 \left(\sigma_N^2 + (v-1) c_{if} \right), \end{aligned} \quad (48)$$

$$c_{D^{(L)}} = -\frac{\sigma_{D^{(L)}}^2}{(v-1)}. \quad (49)$$

Concentration for large m . Since the D 's can be expressed as a sum of different U 's, their concentration for $m \gg 1$ follows directly from that of the U 's.

B.1.3 Estimate of the conditional class probability

We can now turn back to the original problem of estimating

$$f_{i_1 \rightarrow L}^{(1 \rightarrow L)}(\alpha | \mu_1) = \frac{\sum_{\mu_2, \dots, \mu_L=1}^v N_{i_1}^{(1)}(\mu_1; \mu_2) \times \dots \times N_{i_L}^{(L)}(\mu_L; \alpha)}{\sum_{\mu_2, \dots, \mu_L=1}^v \sum_{\mu_{L+1}=1}^{n_c} N_{i_1}^{(1)}(\mu_1; \mu_2) \times \dots \times N_{i_L}^{(L)}(\mu_L; \mu_{L+1})} = \frac{U_{i_1 \rightarrow L}^{(1 \rightarrow L)}(\mu_1; \alpha)}{D_{i_1 \rightarrow L}^{(1 \rightarrow L)}(\mu_1)}. \quad (50)$$

Having shown that both numerator and denominator converge to their average for large m , we can expand for small fluctuations around these averages and write

$$f_{i_{1 \rightarrow L}}^{(1 \rightarrow L)}(\alpha | \mu_1) = \frac{v^{-1} m^L \left(1 + \frac{U_{i_{1 \rightarrow L}}^{(1 \rightarrow L)}(\mu_1; \alpha) - m^L/v}{m^L/v} \right)}{n_c v^{-1} m^L \left(1 + \frac{D_{i_{1 \rightarrow L}}^{(1 \rightarrow L)}(\mu_1) - n_c m^L/v}{m^L} \right)} \quad (51)$$

$$\begin{aligned} &= \frac{1}{n_c} + \frac{1}{n_c} \frac{U_{i_{1 \rightarrow L}}^{(1 \rightarrow L)}(\mu_1; \alpha) - m^L/v}{m^L/v} - \frac{1}{n_c} \frac{D_{i_{1 \rightarrow L}}^{(1 \rightarrow L)}(\mu_1) - n_c m^L/v}{m^L/v} \\ &= \frac{1}{n_c} + \frac{v}{n_c m^L} \left(U_{i_{1 \rightarrow L}}^{(1 \rightarrow L)}(\mu_1; \alpha) - \frac{1}{n_c} D_{i_{1 \rightarrow L}}^{(1 \rightarrow L)}(\mu_1) \right). \end{aligned} \quad (52)$$

Since the conditional frequencies average to n_c^{-1} , the term in brackets averages to zero. We can then estimate the size of the fluctuations of the conditional frequencies (i.e. the ‘signal’) with the standard deviation of the term in brackets.

It is important to notice that, for each L and position $i_{1 \rightarrow L}$, D is the sum over α of U , and the U with different α at fixed low-level feature μ_1 are identically distributed. In general, for a sequence of identically distributed variables $(X_\alpha)_{\alpha=1, \dots, n_c}$,

$$\left\langle \left(\frac{1}{n_c} \sum_{\beta=1}^v X_\beta \right)^2 \right\rangle = \frac{1}{n_c^2} \sum_{\beta=1}^{n_c} \left(\langle X_\beta^2 \rangle + \sum_{\beta' \neq \beta} \langle X_\beta X_{\beta'} \rangle \right) = \frac{1}{n_c} \left(\langle X_\beta^2 \rangle + \sum_{\beta' \neq \beta} \langle X_\beta X_{\beta'} \rangle \right). \quad (53)$$

Hence,

$$\begin{aligned} \left\langle \left(X_\alpha - \frac{1}{n_c} \sum_{\beta=1}^{n_c} X_\beta \right)^2 \right\rangle &= \langle X_\alpha^2 \rangle + n_c^{-2} \sum_{\beta, \gamma=1}^{n_c} \langle X_\beta X_\gamma \rangle - 2n_c^{-1} \sum_{\beta=1}^{n_c} \langle X_\alpha X_\beta \rangle \\ &= \langle X_\alpha^2 \rangle - n_c^{-1} \left(\langle X_\alpha \rangle^2 + \sum_{\beta \neq \alpha} \langle X_\alpha X_\beta \rangle \right) \\ &= \langle X_\alpha^2 \rangle - n_c^{-2} \left\langle \left(\sum_{\beta=1}^{n_c} X_\beta \right)^2 \right\rangle. \end{aligned} \quad (54)$$

In our case

$$\begin{aligned} \left\langle \left(U_{i_{1 \rightarrow L}}^{(1 \rightarrow L)}(\mu_1; \alpha) - \frac{1}{n_c} D_{i_{1 \rightarrow L}}^{(1 \rightarrow L)}(\mu_1) \right)^2 \right\rangle &= \left\langle \left(U_{i_{1 \rightarrow L}}^{(1 \rightarrow L)}(\mu_1; \alpha) \right)^2 \right\rangle - n_c^{-2} \left\langle \left(D_{i_{1 \rightarrow L}}^{(1 \rightarrow L)}(\mu_1) \right)^2 \right\rangle \\ &= \sigma_{U^{(L)}}^2 - n_c^{-2} \sigma_{D^{(L)}}^2, \end{aligned} \quad (55)$$

where, in the second line, we have used that $\langle U^{(L)} \rangle = \langle D^{(L)} \rangle / n_c$ to convert the difference of second moments into a difference of variances. By Eq. (30) and Eq. (47),

$$\begin{aligned} \sigma_{U^{(L)}}^2 - n_c^{-2} \sigma_{D^{(L)}}^2 &= v \sigma_{U^{(L-1)}}^2 (\sigma_N^2 - \sigma_{if}^2) + v \langle U^{(L-1)} \rangle^2 (\sigma_N^2 + (v-1) \sigma_{if}^2) \\ &\quad - \frac{v}{n_c^2} \sigma_{D^{(L-1)}}^2 (\sigma_N^2 - \sigma_{if}^2) - \frac{v}{n_c^2} \langle D^{(L-1)} \rangle^2 (\sigma_N^2 + (v-1) \sigma_{if}^2) \\ &= v (\sigma_N^2 - \sigma_{if}^2) (\sigma_{U^{(L-1)}}^2 - n_c^{-2} \sigma_{D^{(L-1)}}^2), \end{aligned} \quad (56)$$

having used again that $\langle U^{(L)} \rangle = \langle D^{(L)} \rangle / n_c$. Iterating,

$$\sigma_{U^{(L)}}^2 - n_c^{-2} \sigma_{D^{(L)}}^2 = [v (\sigma_N^2 - \sigma_{if}^2)]^{L-1} ((\sigma_{U^{(1)}}^2 - n_c^{-2} \sigma_{D^{(1)}}^2)). \quad (57)$$

Since

$$\begin{aligned}\sigma_{U^{(1)}}^2 &= \frac{m}{v} \frac{v-1}{v} \frac{v^s - m}{v^s - 1} \xrightarrow{v \gg 1} \frac{m}{v}, \\ n_c^{-2} \sigma_{D^{(1)}}^2 &= n_c^{-1} \sigma_N^2 + n_c^{-1} (n_c - 1) \sigma_{if}^2 \xrightarrow{v \gg 1} n_c^{-1} \left(\frac{m}{v} \right)^2 \left(\frac{v}{m} - \frac{n_c}{v^{s-1}} \right) = \frac{1}{n_c} \frac{m}{v} \left(1 - \frac{mn_c}{v^s} \right),\end{aligned}\quad (58)$$

One has

$$\sigma_{U^{(L)}}^2 - n_c^{-2} \sigma_{D^{(L)}}^2 \xrightarrow{v \gg 1} \frac{m^L}{v} \left(1 - \frac{1 - n_c m / v^s}{n_c} \right), \quad (59)$$

so that

$$\text{Var} \left[f_{i_1 \rightarrow L}^{(1 \rightarrow L)}(\alpha | \mu_1) \right] = v^2 \frac{\left\langle \left(U_{i_1 \rightarrow L}^{(1 \rightarrow L)}(\mu_1; \alpha) - \frac{1}{n_c} D_{i_1 \rightarrow L}^{(1 \rightarrow L)}(\mu_1) \right)^2 \right\rangle}{n_c^2 m^{2L}} \xrightarrow{v, n_c \gg 1} \frac{v}{n_c} \frac{1}{n_c m^L}. \quad (60)$$

B.2 Introducing sampling noise due to the finite training set

In a supervised learning setting where only P of the total data are available, the occurrences N are replaced with their empirical counterparts \hat{N} . In particular, the empirical joint occurrence $\hat{N}(\mu; \alpha)$ ⁷ coincides with the number of successes when sampling P points without replacement from a population of P_{\max} where only $N(\mu; \alpha)$ belong to class α and display feature μ in position j . Thus, $\hat{N}(\mu; \alpha)$ obeys a hypergeometric distribution where P plays the role of the number of trials, P_{\max} the population size, and the true occurrence $N(\mu; \alpha)$ the number of favorable cases. If P is large and P_{\max} , $N(\mu; \alpha)$ are both larger than P , then

$$\hat{N}(\mu; \alpha) \rightarrow \mathcal{N} \left(P \frac{N(\mu; \alpha)}{P_{\max}}, P \frac{N(\mu; \alpha)}{P_{\max}} \left(1 - \frac{N(\mu; \alpha)}{P_{\max}} \right) \right), \quad (61)$$

where the convergence is meant as a convergence in probability and $\mathcal{N}(a, b)$ denotes a Gaussian distribution with mean a and variance b . The statement above holds when the ratio $N(\mu; \alpha)/P_{\max}$ is away from 0 and 1, which is true with probability 1 for large v due to the concentration of $f(\alpha|\mu)$. In complete analogy, the empirical occurrence $\hat{N}(\mu)$ obeys

$$\hat{N}(\mu) \rightarrow \mathcal{N} \left(P \frac{N(\mu)}{P_{\max}}, P \frac{N(\mu)}{P_{\max}} \left(1 - \frac{N(\mu)}{P_{\max}} \right) \right). \quad (62)$$

We obtain the empirical conditional frequency by the ratio of Eq. (61) and Eq. (62). Since $N(\mu) = P_{\max}/v$ and $f(\alpha|\mu) = N(\mu; \alpha)/N(\mu)$, we have

$$\hat{f}(\alpha|\mu) = \frac{\frac{f(\alpha|\mu)}{v} + \xi_P \sqrt{\frac{1}{P} \frac{f(\alpha|\mu)}{v} \left(1 - \frac{f(\alpha|\mu)}{v} \right)}}{\frac{1}{v} + \zeta_P \sqrt{\frac{1}{P} \frac{1}{v} \left(1 - \frac{1}{v} \right)}}, \quad (63)$$

where ξ_P and ζ_P are correlated zero-mean and unit-variance Gaussian random variables over independent drawings of the P training points. By expanding the denominator of the right-hand side for large P we get, after some algebra,

$$\hat{f}(\alpha|\mu) \simeq f(\alpha|\mu) + \xi_P \sqrt{\frac{v f(\alpha|\mu)}{P} \left(1 - \frac{f(\alpha|\mu)}{v} \right)} - \zeta_P f(\alpha|\mu) \sqrt{\frac{v}{P} \left(1 - \frac{1}{v} \right)}. \quad (64)$$

Recall that, in the limit of large n_c and m , $f(\alpha|\mu) = n_c^{-1} (1 + \sigma_f \xi_{\text{RHM}})$ where ξ_{RHM} is a zero-mean and unit-variance Gaussian variable over the realizations of the RHM, while σ_f is the ‘signal’, $\sigma_f^2 = v/m^L$ by Eq. (60). As a result,

$$\hat{f}(\alpha|\mu) \xrightarrow{n_c, m, P \gg 1} \frac{1}{n_c} \left(1 + \sqrt{\frac{v}{m^L}} \xi_{\text{RHM}} + \sqrt{\frac{vn_c}{P}} \xi_P \right). \quad (65)$$

⁷For ease of notation, we drop level and positional indices in this subsection.

B.3 Sample complexity

From Eq. (65) it is clear that for the ‘signal’ \hat{f} , the fluctuations due to noise must be smaller than those due to the random choice of the composition rules. Therefore, the crossover takes place when the two nose terms have the same size, occurring at $P = P_c$ such that

$$\sqrt{\frac{v}{m^L}} = \sqrt{\frac{vn_c}{P_c}} \Rightarrow P_c = n_c m^L. \quad (66)$$

C One-Step Gradient Descent (GD)

In this section, we consider a simple gradient-descent setting that allows us to demonstrate that P_c coincides with the number of training examples required to learn a synonymic invariant representation. In this setting, we first generate an instance of the RHM, then train a one-hidden-layer fully-connected network on the first s -dimensional patch of the input data. Since many data have the same first s -dimensional patch but a different label, this network cannot fit the data. Nevertheless, in the case where the s -dimensional patches are orthogonalized, neural networks can learn the synonymic invariance of the RHM if trained on at least P_c data.

GD on Cross-Entropy Loss. More specifically, let us first sample an instance of the RHM, then P input-label pairs (\mathbf{x}_k, α_k) with $\alpha_k := \alpha(\mathbf{x}_k)$ for all $k = 1, \dots, P$. For any datum \mathbf{x} , we denote with $\boldsymbol{\mu}_1(\mathbf{x})$ the s -tuple of features in the first patch and with $\boldsymbol{\delta}_\mu$ the one-hot encoding of the s -tuple $\boldsymbol{\mu}$ (with dimension v^s). The fully-connected network acts on the one-hot encoding of the s -tuples with ReLU activations $\sigma(x) = \max(0, x)$,

$$\mathcal{F}_{\text{NN}}(\boldsymbol{\delta}_\mu) = \frac{1}{H} \sum_{h=1}^H a_h \sigma(\mathbf{w}_h \cdot \boldsymbol{\delta}_\mu), \quad (67)$$

where the inner-layer weights \mathbf{w}_h ’s have the same dimension as $\boldsymbol{\delta}_\mu$ and the top-layer weights a_h ’s are n_c -dimensional. The top-layer weights are initialized as i.i.d. Gaussian with zero mean and unit variance and fixed. The \mathbf{w}_h ’s are trained by Gradient Descent (GD) on the cross-entropy loss,

$$\mathcal{L} = \hat{\mathbb{E}}_{\boldsymbol{\delta}} \left[- \sum_{\beta=1}^{n_c} \delta_{\beta, \alpha(\mathbf{x})} \log \left(\frac{e^{(\mathcal{F}_{\text{NN}}(\boldsymbol{\delta}))_{\beta}}}{\sum_{\beta'=1}^{n_c} e^{(\mathcal{F}_{\text{NN}}(\boldsymbol{\delta}))_{\beta'}}} \right) \right], \quad (68)$$

where $\delta_{\beta, \alpha(\mathbf{x})}$ stems from the one-hot encoding of the class label $\alpha(\mathbf{x})$ and $\hat{\mathbb{E}}$ denotes expectation over the training set. For simplicity, we consider the mean-field limit $H \rightarrow \infty$, so that $\mathcal{F}_{\text{NN}}^{(0)} = 0$ identically, and initialize all the inner-layer weights to $\mathbf{1}$ (the vector with all elements set to 1).

Update of the Hidden Representation. In this setting, with enough training points, one step of gradient descent is sufficient to build a representation invariant to the exchange of synonyms. Due to the one-hot encoding, $(\mathbf{w}_h \cdot \boldsymbol{\delta}_\mu)$, namely the h -th component of the hidden representation of the s -tuple $\boldsymbol{\mu}$, coincides with the μ -th component of the weight \mathbf{w}_h . This component, which is set to 1 at initialization, is updated by (minus) the corresponding component of the gradient of the loss in Eq. (68). Recalling that at initialization the predictor is 0 and all the components of the inner-layer weights are 1, we get (cf. Eq. (10) of the main text)

$$\Delta f_h(\boldsymbol{\mu}) = -\nabla_{(\mathbf{w}_h)_\mu} \mathcal{L} = \frac{1}{P} \sum_{\alpha=1}^{n_c} a_{h, \alpha} \left(\hat{N}_1(\boldsymbol{\mu}; \alpha) - \frac{1}{n_c} \hat{N}_1(\boldsymbol{\mu}) \right), \quad (69)$$

where $\hat{N}_1(\boldsymbol{\mu})$ is the empirical occurrence of the s -tuple $\boldsymbol{\mu}$ in the first patch of the P training points and $\hat{N}_1(\boldsymbol{\mu}; \alpha)$ is the (empirical) joint occurrence of the s -tuple $\boldsymbol{\mu}$ and the class label α . As P increases, the empirical occurrences \hat{N} converge to the true occurrences N , which are invariant for the exchange of synonym s -tuples $\boldsymbol{\mu}$. Hence, the hidden representation is also invariant for the exchange of synonym s -tuples in this limit.

C.1 Extension to a one-hidden-layer CNN

The same argument can be carried out by considering a one-hidden-layer CNN with weight sharing and global average pooling:

$$\mathcal{F}_{\text{CNN}}(\mathbf{x}) = \frac{1}{H s^{L-1}} \sum_{h=1}^H \sum_{j=1}^{s^{L-1}} \mathbf{a}_h \sigma(\mathbf{w}_h \cdot \mathbf{x}_j), \quad (70)$$

where we added an average over all the input patches j . The gradient updates now read,

$$-\nabla_{(\mathbf{w}_h)_\mu} \mathcal{L} = \frac{1}{P} \sum_{\alpha=1}^{n_c} a_{h,\alpha} \frac{1}{s^{L-1}} \sum_{j=1}^{s^{L-1}} \left(\hat{N}_j(\boldsymbol{\mu}; \alpha) - \frac{1}{n_c} \hat{N}_j(\boldsymbol{\mu}) \right), \quad (71)$$

hence, synonymic invariance can now be inferred from the average occurrences over patches. This average results in a reduction of both the signal and noise term by the same factor $\sqrt{s^{L-1}}$. Consequently, analogously to the case without weight sharing, the hidden representation becomes insensitive to the exchange of synonymic features for $P \gg P_c = n_c m^L$. We conclude that weight sharing does not change the sample complexity in this setting.

D Improved Sample Complexity via Clustering

In [Section 3](#) of the main text and [Supplementary Section C](#), we showed that the hidden representation of a one-hidden layer fully-connected network trained on the first patch of the RHM inputs becomes insensitive to exchanges of synonyms at $P = P^* = P_c = n_c m^L$. In this section, we consider the maximal dataset case $n_c = v$ and $m = v^{s-1}$, and show that a distance-based clustering method acting on these hidden representations would identify synonyms at $P \simeq \sqrt{n_c} m^L$, much smaller than P_c in the large- n_c limit. This study is relevant for algorithms that intercalate clustering steps to usual gradient descent, such as the algorithms introduced in [\[1, 2\]](#).

Let us then imagine feeding the representations updates $\Delta f_h(\boldsymbol{\mu})$ of [Eq. \(69\)](#) to a clustering algorithm aimed at identifying synonyms. This algorithm is based on the distance between the representations of different tuples of input features $\boldsymbol{\mu}$ and $\boldsymbol{\nu}$,

$$\|\Delta f(\boldsymbol{\mu}) - \Delta f(\boldsymbol{\nu})\|^2 := \frac{1}{H} \sum_{h=1}^H (\Delta f_h(\boldsymbol{\mu}) - \Delta f_h(\boldsymbol{\nu}))^2, \quad (72)$$

where H is the number of hidden neurons. By defining

$$\hat{g}_\alpha(\boldsymbol{\mu}) := \frac{\hat{N}_1(\boldsymbol{\mu}; \alpha)}{P} - \frac{1}{n_c} \frac{\hat{N}_1(\boldsymbol{\mu})}{P}, \quad (73)$$

and denoting with $\hat{\mathbf{g}}(\boldsymbol{\mu})$ the n_c -dimensional sequence having the \hat{g}_α 's as components, we have

$$\begin{aligned} \|\Delta f(\boldsymbol{\mu}) - \Delta f(\boldsymbol{\nu})\|^2 &= \sum_{\alpha, \beta=1}^{n_c} \left(\frac{1}{H} \sum_h a_{h,\alpha} a_{h,\beta} \right) (\hat{g}_\alpha(\boldsymbol{\mu}) - \hat{g}_\alpha(\boldsymbol{\nu})) (\hat{g}_\beta(\boldsymbol{\mu}) - \hat{g}_\beta(\boldsymbol{\nu})) \\ &\xrightarrow{H \rightarrow \infty} \sum_{\alpha=1}^{n_c} (\hat{g}_\alpha(\boldsymbol{\mu}) - \hat{g}_\alpha(\boldsymbol{\nu}))^2 = \|\hat{\mathbf{g}}(\boldsymbol{\mu}) - \hat{\mathbf{g}}(\boldsymbol{\nu})\|^2, \end{aligned} \quad (74)$$

where we used the i.i.d. Gaussian initialization of the readout weights to replace the sum over neurons with $\delta_{\alpha,\beta}$.

Due to the sampling noise, from [Eq. \(61\)](#) and [Eq. \(62\)](#), when $1 \ll P \ll P_{\max}$,

$$\hat{g}_\alpha(\boldsymbol{\mu}) = g_\alpha(\boldsymbol{\mu}) + \sqrt{\frac{1}{n_c m v P}} \eta_\alpha(\boldsymbol{\mu}), \quad (75)$$

where $\eta_\alpha(\boldsymbol{\mu})$ is a zero-mean and unit-variance Gaussian noise and g without hat denotes the $P \rightarrow P_{\max}$ limit of \hat{g} . In the limit $1 \ll P \ll P_{\max}$, the noises with different α and $\boldsymbol{\mu}$ are independent of each other. Thus,

$$\|\hat{\mathbf{g}}(\boldsymbol{\mu}) - \hat{\mathbf{g}}(\boldsymbol{\nu})\|^2 = \|\mathbf{g}(\boldsymbol{\mu}) - \mathbf{g}(\boldsymbol{\nu})\|^2 + \frac{1}{n_c m v P} \|\boldsymbol{\eta}(\boldsymbol{\mu}) - \boldsymbol{\eta}(\boldsymbol{\nu})\|^2 + \frac{2}{\sqrt{n_c m v P}} (\mathbf{g}(\boldsymbol{\mu}) - \mathbf{g}(\boldsymbol{\nu})) \cdot (\boldsymbol{\eta}(\boldsymbol{\mu}) - \boldsymbol{\eta}(\boldsymbol{\nu})). \quad (76)$$

If $\boldsymbol{\mu}$ and $\boldsymbol{\nu}$ are synonyms, then $\mathbf{g}(\boldsymbol{\mu}) = \mathbf{g}(\boldsymbol{\nu})$ and only the noise term contributes to the right-hand side of Eq. (76). If this noise is sufficiently small, then the distance above can be used to cluster tuples into synonymic groups.

By the independence of the noises and the Central Limit Theorem, for $n_c \gg 1$,

$$\|\boldsymbol{\eta}(\boldsymbol{\mu}) - \boldsymbol{\eta}(\boldsymbol{\nu})\|^2 \sim \mathcal{N}(2n_c, \mathcal{O}(\sqrt{n_c})), \quad (77)$$

over independent samplings of the P training points. The g 's are also random variables over independent realizations of the RHM with zero mean and variance proportional to the variance of the conditional probabilities $f(\alpha|\boldsymbol{\mu})$ (see Eq. (51) and Eq. (60)),

$$\text{Var}[g_\alpha(\boldsymbol{\mu})] = \frac{1}{n_c m v n_c m^L} = \frac{1}{n_c m v P_c}. \quad (78)$$

To estimate the size of $\|\mathbf{g}(\boldsymbol{\mu}) - \mathbf{g}(\boldsymbol{\nu})\|^2$ we must take into account the correlations (over RHM realizations) between g 's with different class label and tuples. However, in the maximal dataset case $n_c = v$ and $m = v^{s-1}$, both the sum over classes and the sum over tuples of input features of the joint occurrences $N(\boldsymbol{\mu}; \alpha)$ are fixed deterministically. The constraints on the sums allow us to control the correlations between occurrences of the same tuple within different classes and of different tuples within the same class, so that the size of the term $\|\mathbf{g}(\boldsymbol{\mu}) - \mathbf{g}(\boldsymbol{\nu})\|^2$ for $n_c = v \gg 1$ can be estimated via the Central Limit Theorem:

$$\|\mathbf{g}(\boldsymbol{\mu}) - \mathbf{g}(\boldsymbol{\nu})\|^2 \sim \mathcal{N}\left(\frac{2n_c}{n_c m v P_c}, \frac{\mathcal{O}(\sqrt{n_c})}{n_c m v P_c}\right). \quad (79)$$

The mixed term $(\mathbf{g}(\boldsymbol{\mu}) - \mathbf{g}(\boldsymbol{\nu})) \cdot (\boldsymbol{\eta}(\boldsymbol{\mu}) - \boldsymbol{\eta}(\boldsymbol{\nu}))$ has zero average (both with respect to training set sampling and RHM realizations) and can also be shown to lead to relative fluctuations of order $\mathcal{O}(\sqrt{n_c})$ in the maximal dataset case.

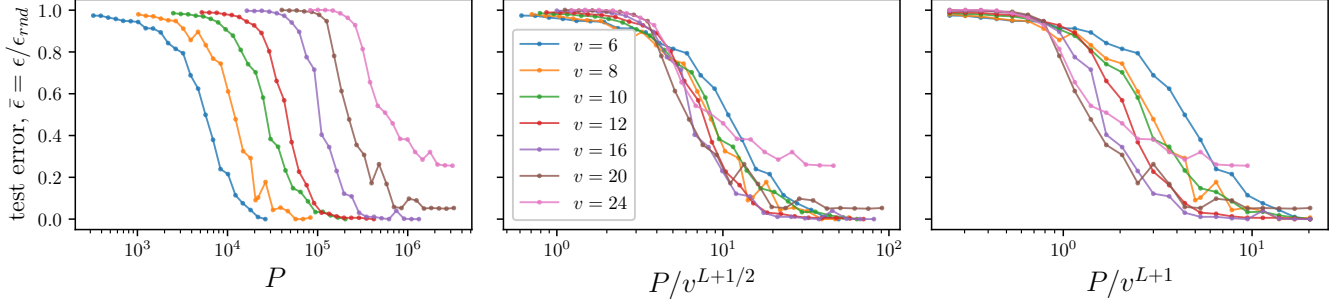
To sum up, we have that, for synonyms,

$$\|\hat{\mathbf{g}}(\boldsymbol{\mu}) - \hat{\mathbf{g}}(\boldsymbol{\nu})\|^2 = \|\boldsymbol{\eta}(\boldsymbol{\mu}) - \boldsymbol{\eta}(\boldsymbol{\nu})\|^2 \sim \frac{1}{m v P} \left(1 + \frac{1}{\sqrt{n_c}} \xi_P\right), \quad (80)$$

where ξ_P is some $\mathcal{O}(1)$ noise dependent on the training set sampling. If $\boldsymbol{\mu}$ and $\boldsymbol{\nu}$ are not synonyms, instead,

$$\|\hat{\mathbf{g}}(\boldsymbol{\mu}) - \hat{\mathbf{g}}(\boldsymbol{\nu})\|^2 \sim \frac{1}{m v P} \left(1 + \frac{1}{\sqrt{n_c}} \xi_P\right) + \frac{1}{m v P_c} \left(1 + \frac{1}{\sqrt{n_c}} \xi_{\text{RHM}}\right), \quad (81)$$

where ξ_{RHM} is some $\mathcal{O}(1)$ noise dependent on the RHM realization. In this setting, the signal is the deterministic part of the difference between representations of non-synonymic tuples. Due to the sum over class labels, the signal is scaled up by a factor n_c , whereas the fluctuations (stemming from both sampling and model) are only increased by $\mathcal{O}(\sqrt{n_c})$. Therefore, the signal required for clustering emerges from the sampling noise at $P = P_c / \sqrt{n_c} = \sqrt{n_c} m^L$, equal to $v^{1/2+L(s-1)}$ in the maximal dataset case. This prediction is tested for $s = 2$ in [Supplementary Fig. 1](#), which shows the error achieved by a layerwise algorithm which alternates single GD steps to clustering of the resulting representations [1, 2]. More specifically, the weights of the first hidden layer are updated with a single GD step while keeping all the other weights frozen. The resulting representations are then clustered, so as to identify groups of synonymic level-1 tuples. The centroids of the ensuing clusters, which correspond to level-2 features, are orthogonalized and used as inputs of another one-step GD protocol, which aims at identifying synonymic tuples of level-2 features. The procedure is iterated L times.



Supplementary Figure 1: **Sample complexity for layerwise training**, $m = n_c = v$, $L = 3$, $s = 2$. Training of a L -layers network is performed layerwise by alternating one-step GD as described in Section 4.C and clustering of the hidden representations. Clustering of the $mv = v^2$ representations for the different one-hot-encoded input patches is performed with the k -means algorithms. Clustered representations are then orthogonalized and the result is given to the next one-step GD procedure. Left: Test error vs. number of training points. Different colors correspond to different values of v . Center: collapse of the test error curves when rescaling the x -axis by $v^{L+1/2}$. Right: analogous, when rescaling the x -axis by v^{L+1} . The curves show a better collapse when rescaling by $v^{L+1/2}$, suggesting that these layerwise algorithms as an advantage of a factor \sqrt{v} over end-to-end training with deep CNNs, for which $P^* = v^{L+1}$.

E Instances of the Random Hierarchy Model With No Correlations

Given that the rules in the RHM are chosen uniformly at random, there is a small probability of sampling an instance of the model with no input-output correlations. For these instances, it would be impossible to use the mechanism illustrated in this work to learn semantic invariance and good generalization from correlations. In this section, we show that the probability of sampling such specific instances of the RHM vanishes as the number of synonyms m is increased.

E.1 Maximal case $n_c = v$ and $m = v^{s-1}$

The number of possible RHMs with L layers and generic values of v , m and n_c is given by

$$\#\{\text{RHMs}\} = \frac{(v^s)!}{(m!)^{n_c} (v^s - mn_c)!} \left(\frac{(v^s)!}{(m!)^v (v^s - mv)!} \right)^{L-1} \left(\frac{1}{v!} \right)^{L-1}, \quad (82)$$

which is easily determined by recalling that an instance of the RHM consists of L composition rules, chosen uniformly at random among all the possible allocations of m s -dimensional low-level representations to each of the v high-level features (or to the n_c labels at the highest level). The additional factor of $(v!)^{1-L}$ is due to the invariance of the RHM for relabelling of the hidden features. For $n_c = v$ and $m = v^{s-1}$, $\#\{\text{RHMs}\}$ becomes $\binom{v^s}{v^{s-1} \dots v^{s-1}}^L \left(\frac{1}{v!} \right)^{L-1}$. The instances without input-output correlations are defined by having $N_i^{(\ell)}(\mu_\ell; \mu_{\ell+1}) = v^{s-2}$ for each layer ℓ independently of μ_ℓ and $\mu_{\ell+1}$. The number of such rules can be computed as follows. Let us consider a given high-level feature, e.g. the symbol 1. We want to assign to it $m = v^{s-1}$ s -tuples

$$(1, \alpha_1^{1,1}, \dots, \alpha_1^{1,s-1}), \dots, (1, \alpha_{v^{s-2}}^{1,1}, \dots, \alpha_{v^{s-2}}^{1,s-1}), \dots, (v, \alpha_{v^{s-1} - (v^{s-2}-1)}^{1,1}, \dots, \alpha_{v^{s-1} - (v^{s-2}-1)}^{1,s-1}), \dots, (v, \alpha_{v^{s-1}}^{1,1}, \dots, \alpha_{v^{s-1}}^{1,s-1}), \quad (83)$$

where the first v^{s-2} tuples has as first symbol 1, the second v^{s-2} the symbol 2 and we continue up to the last v^{s-2} tuples with first symbol v . The numbers $\{\alpha_i^{1,t}\}_{i=1, \dots, v^{s-1}}$ are permutations of the set $\{1, \dots, v\}^{v^{s-2}}$ for feature 1 and location t . In these rules, there is no symbol that occurs more than the others at a given location. Consequently, the network cannot exploit any correlation between the presence of a symbol at a given location and the label to solve the task. With regard to the other features j of the previous layer, to any of these we will assign the v^{s-1} tuples $(1, \alpha_1^{j,1}, \dots, \alpha_1^{j,s-1}), \dots, (v, \alpha_{v^{s-1}}^{j,1}, \dots, \alpha_{v^{s-1}}^{j,s-1})$, with the numbers $\{\alpha_i^{j,t}\}$ being the same of $\alpha_i^{1,t}$ for any t but shifted forward of $(j-1)v$ positions. For example, the numbers related to the “block” of tuples with first element 1 for feature 1 will be the same related to the “block” of tuples with first element 2 for feature. In formulae: $\alpha_i^{j,t} = \alpha_{i-(j-1)v}^{1,t}$, with $i - (j-1)v$

being equivalent to $(v^{s-1} - (v - i) + 1)$ (periodic boundary conditions). The number of such uncorrelated rules is just the number $(v^{s-1})!$ of permutations of the numbers $\{\alpha_i^{1,t}\}_{i=1,\dots,v^{s-1}}$ for a fixed tuple location t , elevated to the number of positions $s - 1$. Consequently, the fraction of uncorrelated rules for L layers is:

$$f_{\text{uncorr}} = \frac{1}{v!} \left(\frac{(v^{s-1})^{(s-1)}}{\binom{v^s}{v^{s-1}\dots v^{s-1}} \frac{1}{v!}} \right)^L. \quad (84)$$

We now want to show that f_{uncorr} vanishes for large v . By approximating the factorials in (84) via Stirling's approximation, we get

$$f_{\text{uncorr}} \approx \frac{1}{v!} \left(\frac{v^{(s-1)(v^{s-1} + \frac{1}{2})} e^{-v^{s-1}(s-1)}}{v^{s(v^s + \frac{1}{2})} e^{-v^s}} v^{v^{(s-1)(v^{s-1} + \frac{1}{2})}} e^{-v^s} \right)^L, \quad (85)$$

yielding the following limit behavior for large v :

$$f_{\text{uncorr}} \approx \frac{1}{v!} \left(\frac{e^{-v^{s-1}(s-1)}}{v^{v^s}} \right)^L, \quad (86)$$

which is vanishing for large v and large L .

E.2 Generic m case

Let's characterize the uncorrelated rules in the case of generic m . For each single-layer rule, we assign m s -tuples to each symbol of the previous layer. Let's consider a given symbol j . To this symbol, we assign m s -tuples of the type $(\alpha_1^{j,1}, \dots, \alpha_1^{j,s}), (\alpha_2^{j,1}, \dots, \alpha_2^{j,s}), \dots, (\alpha_m^{j,1}, \dots, \alpha_m^{j,s})$, with the m numbers $(\alpha_i^{j,t})_i$ at fixed location t being a permutation of a subset of $\{1, \dots, v\}^{v^{s-2}}$ such that, if we call m_q the number of items in the subset equal to $q \in \{1, \dots, v\}$, each m_q is either 0 or we have that $m_{q_1} = m_{q_2}$ for q_1 and q_2 such that $m_{q_1} = m_{q_2} > 0$ and $\sum_{q=1}^v m_q = m$. Moreover, since each symbol q can appear at most v^{s-2} times, we have that $m_q \leq v^{s-2}$. We take the m numbers $(\alpha_i^{j,1})_{i=1,\dots,m}$ at the first location $t = 1$ ordered in increasing order. Note that these tuples can be picked just once across different symbols j , imposing then constraints on the numbers $\alpha_i^{j,t}$ for different features j .

As in the case $m = v^{s-1}$ of [Supplementary Subsection E.1](#), we want to show that the probability of occurrence f_{uncorr} of such uncorrelated rules, given by the number of these rules divided by the number of total rules, is vanishing for large v and/or large L . To count the number of uncorrelated rules, that we call $\#_{\text{uncorr}}$, we first count the number $\#_{j,t}$ of possible series of numbers $\{\alpha_i^{f,t}\}_{i=1,\dots,m}$ for a fixed feature j and position $t > 1$, and for a single-layer rule. In other words, we have to count the number of possible subsets made by m elements of $\{1, \dots, v\}^{v^{s-2}}$ such that each symbol $q \in \{1, \dots, v\}$ appears m_q times, with the m_q satisfying the constraints above. We introduce the quantity v_0 which is the number of symbols q which appear 0 times in a given subset. Once we fix v_0 , from the constraint $\sum_{q=1}^v m_q = m$ we get that the features with $m_q > 0$ appear $\bar{m} = \frac{m}{v-v_0}$ if $\frac{m}{v-v_0}$ is a positive integer, otherwise, there are no subsets with that v_0 . Consequently, the number $\#_{j,t}$ is given by:

$$\#_{j,t} = \sum_{v_0=0}^{v-1} \binom{v}{v_0} \mathbb{I} \left[\frac{m}{v-v_0} \in \mathbb{N}_{>0} \right] \mathbb{I} \left[\frac{m}{v-v_0} \leq v^{s-2} \right] m!, \quad (87)$$

where (i) $\binom{v}{v_0}$ counts the number of choices of the features with 0 appearances and (ii) $m!$ counts the number of permutations of the m numbers $\{\alpha_i^{j,t}\}_i$. Since we are interested in proving that f_{uncorr} is vanishing for large v and L , we upper bound it relaxing the constraint that $\frac{m}{v-v_0} \in \mathbb{N}_{>0}$ and using that $\binom{v}{v_0} \leq \binom{v}{\lceil v/2 \rceil}$:

$$\#_{j,t} \leq \left(v - \frac{m}{v^{s-2}} \right) \binom{v}{\lceil v/2 \rceil} m! \quad (88)$$

Considering all the s locations, we get

$$\#_j \leq \left(v - \frac{m}{v^{s-2}} \right)^s \binom{v}{\lceil v/2 \rceil}^s (m!)^{s-1}, \quad (89)$$

where $\#_j$ is defined similarly as $\#_{f,t}$. Notice that for the first location $t = 1$ there is not a factor $m!$ since we are ordering the numbers $\alpha_i^{j,1}$ in ascending order there.

If we want to count $\#_{\text{uncorr}}$, we have to take into account that we are sampling without replacement from the space of s -tuples, and hence two different symbols j cannot share the same s -tuples, hence increasing the number of possible rules. To upper bound $\#_{\text{uncorr}}$, we relax this constraint, hence sampling the tuples with replacement. Consequently, we have:

$$\#_{\text{uncorr}} \leq \left[\left(v - \frac{m}{v^{s-2}} \right)^s \binom{v}{\lceil v/2 \rceil}^s (m!)^{s-1} \right]^v, \quad (90)$$

since the choice of the $\alpha_i^{j,t}$ is independent between different features j . Consequently for a L -layer rule:

$$f_{\text{uncorr}} \leq \left[\left(v - \frac{m}{v^{s-2}} \right)^s \binom{v}{\lceil v/2 \rceil}^s (m!)^{s-1} \right]^{vL} \bigg/ \left[\binom{v^s}{m \dots m}^L \left(\frac{1}{v!} \right)^{L-1} \right] \quad (91)$$

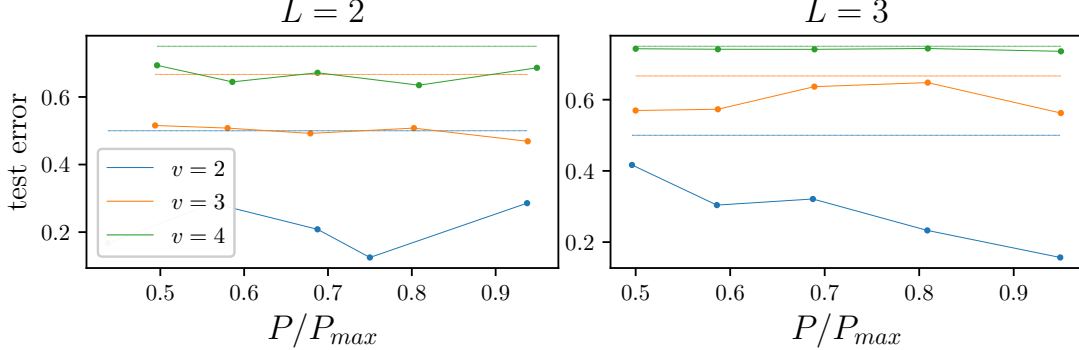
We now assume $m \sim v^\alpha$, with $0 < \alpha < (s-1)$ and for large n we implement the Stirling approximation⁸, getting:

$$f_{\text{uncorr}} \leq \frac{1}{v!} \left(v - v^{\alpha-(s-2)} \right)^{svL} 2^{(v+1)vL} v^{\alpha(v^\alpha+1/2)(s-1)vL+vL/2} e^{-v^\alpha(s-1)vL-vL} \bigg/ v^{L(v^s+v/2-sv/2+s/2)} e^{-\frac{L}{2v^{s-1}}(v(v^\alpha-v^{s-1})+(v^s-v^{1+\alpha}-v^{s-1}))} \quad (92)$$

where we approximated $\lceil v/2 \rceil$ with $v/2$. At the leading order for large v we get, using the fact that $(\alpha+1) < s$

$$f_{\text{uncorr}} \leq \frac{1}{v!} \frac{e^{-(s-1)Lv^{\alpha+1}}}{v^{(v^s)L}} 2^{(v+1)vL}, \quad (93)$$

hence the probability of occurrence of a parity-like rule is vanishing for large n and L .



Supplementary Figure 2: Test error of deep CNNs trained on RHM instances with no correlations, for $s=2$ and $m=n_c=v$ with different v and L . Horizontal dashed lines stand $\epsilon_{\text{rand}} = 1 - v^{-1}$, given by guessing the label uniformly at random. The performance remains close to that of random guess, especially when increasing v .

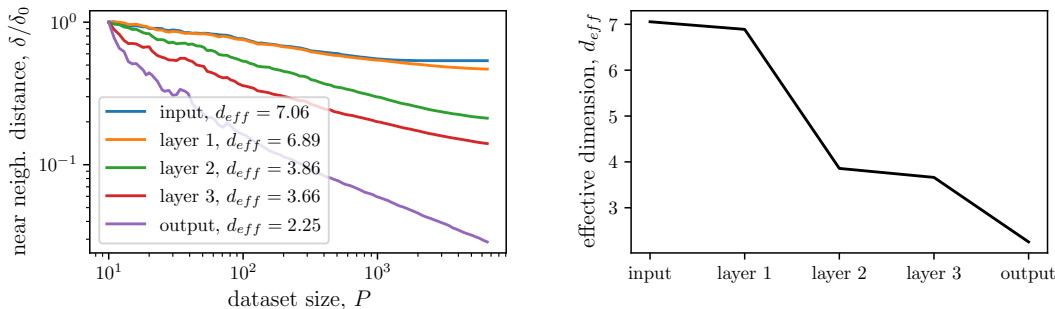
F Intrinsic Dimensionality of Data Representations

In deep learning, the representation of data at each layer of a network can be thought of as lying on a manifold in the layer's activation space. Measures of the *intrinsic dimensionality* of these manifolds can provide insights into how the networks lower the dimensionality of the problem layer by layer. However, such measurements have challenges. One key challenge is that it assumes that real data exist on a smooth manifold, while in practice, the dimensionality is estimated based on a discrete set of points. This leads to counter-intuitive results such as an increase in the intrinsic dimensionality

⁸The Stirling approximation for the multinomial $\binom{n}{a_1 \dots a_k}$ for $n \rightarrow \infty$ and integers a_i such that $\sum_{i=1}^k a_i = n$ is given by $\binom{n}{a_1 \dots a_k} \sim (2\pi n)^{(1/2-k/2)} k^{n+k/2} \exp\{-\frac{k}{2n} \sum_{i=1}^k (a_i - n/k)^2\}$. In our case $n = v^s$, $k = (v+1)$ and $a_i = m$ for $i \in 1, \dots, v$ and $a_{k+1} = (v^s - vm)$.

with depth, especially near the input. An effect that is impossible for continuous smooth manifolds. We resort to an example to illustrate how this increase with depth can result from spurious effects. Consider a manifold of a given intrinsic dimension that undergoes a transformation where one of the coordinates is multiplied by a large factor. This operation would result in an elongated manifold that appears one-dimensional. The measured intrinsic dimensionality would consequently be one, despite the higher dimensionality of the manifold. In the context of neural networks, a network that operates on such an elongated manifold could effectively 'reduce' this extra, spurious dimension. This could result in an increase in the observed intrinsic dimensionality as a function of network depth, even though the actual dimensionality of the manifold did not change.

In the specific case of our data, the intrinsic dimensionality of the internal representations of deep CNNs monotonically decreases with depth, see [Supplementary Fig. 3](#), consistently with the idea proposed in the main text that the CNNs solve the problem by reducing the effective dimensionality of data layer by layer. We attribute this monotonicity to the absence of spurious or noisy directions that might lead to the counter-intuitive effect described above.



Supplementary Figure 3: Effective dimension of the internal representation of a CNN trained on one instance of the RHM with $m = n_c = v, L = 3$ resulting in $P_{\max} = 6'232$. Left: average nearest neighbor distance of input or network activations when probing them with a dataset of size P . The value reported on the y -axis is normalized by $\delta_0 = \delta(P = 10)$. The slope of $\delta(P)$ is used as an estimate of the effective dimension. Right: effective dimension as a function of depth. We observe a monotonic decrease, consistent with the idea that the dimensionality of the problem is reduced by DNNs with depth.

G Additional Results on Sample Complexity

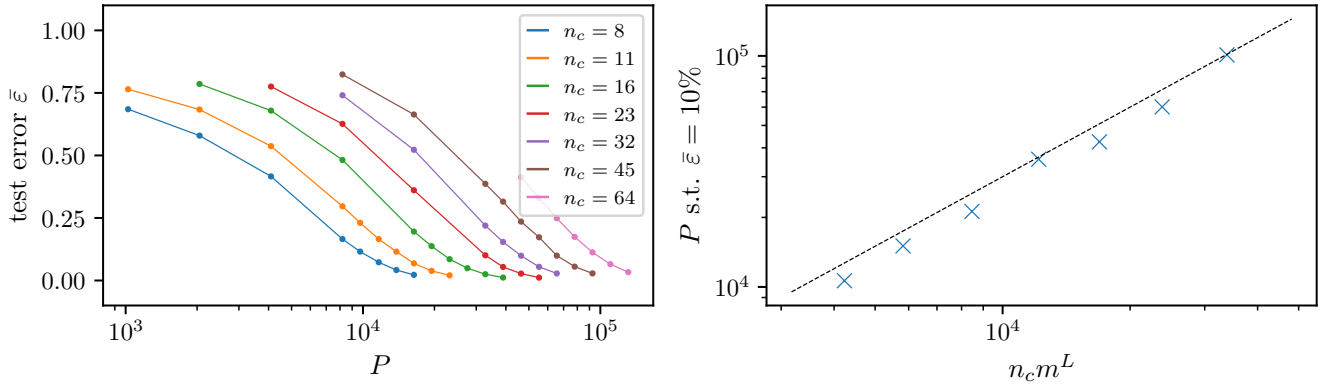
This section collects additional results on the sample complexity of deep networks trained on the RHM ([Supplementary Fig. 4](#) and [Supplementary Fig. 5](#)) and for a ResNet18 trained on different sub-samples of the benchmark dataset CIFAR10 as a function of the sample size ([Supplementary Fig. 6](#)).

[Supplementary Fig. 4](#) shows the behaviour of the sample complexity with varying number of classes n_c when all the other parameters of the RHM are fixed, confirming the linear scaling discussed in the main text.

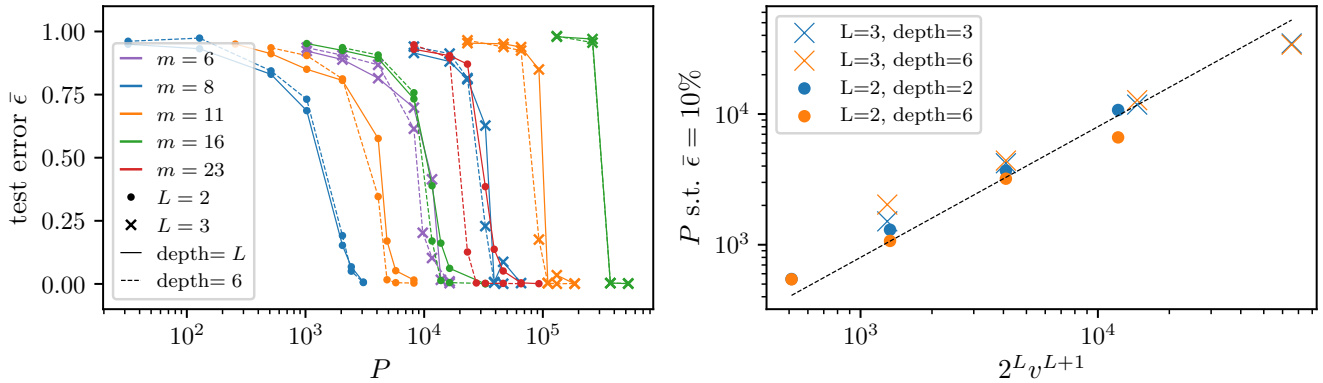
[Supplementary Fig. 5](#) shows the behaviour of the sample complexity for deep fully-connected networks having depth larger than $L + 1$, which are not tailored to the structure of the RHM. Notice that changing architecture seems to induce an additional factor of 2^L to the sample complexity, independent of v, n_c and m . This factor is also polynomial in the input dimension.

References

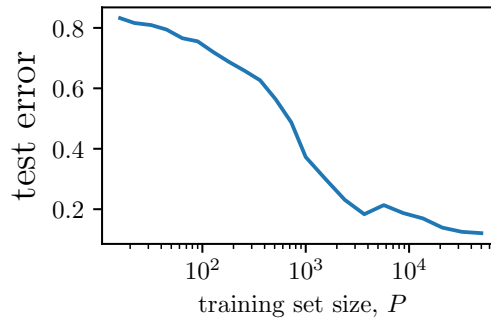
1. Malach, E. & Shalev-Shwartz, S. A Provably Correct Algorithm for Deep Learning that Actually Works. *Preprint at <http://arxiv.org/abs/1803.09522>*. (2018).
2. Malach, E. & Shalev-Shwartz, S. The implications of local correlation on learning some deep functions. *Advances in Neural Information Processing Systems* **33**, 1322–1332 (2020).



Supplementary Figure 4: **Sample complexity of deep CNNs, for $L = s = 2$, $v = 256$, $m = 23$ and different values of n_c .** Left: Test error vs. number of training points with the color indicating the number of classes (see key). Right: sample complexity P^* (crosses) and law $P^* = n_c m^L$ (black dashed).



Supplementary Figure 5: **Sample complexity of deep fully-connected networks with different depth, for $s = 2$ and $m = n_c = v$.** Left: Test error vs. number of training points. The color denotes the value of $m = n_c = v$, the marker the hierarchy depth of the RHM L . Solid lines represent networks having depth L , while dashed lines correspond to networks with depth $6 > L$. Notice that, in all cases, the behaviour of the test error is roughly independent of the network depth. Right: sample complexity P^* (crosses and circles). With respect to the case of deep CNNs tailored to the structure to the RHM, the sample complexity of generic deep networks seems to display an additional factor of 2^L independently of n_c , m and v .



Supplementary Figure 6: **Test error vs. number of training points for a ResNet18 trained on subsamples of the CIFAR10 dataset.** Results are the average of 10 jointly different initializations of the networks and dataset sampling.